Published in final edited form as:
Dev Biol. 2012 May 15; 365(2): 395–413. doi:10.1016/j.ydbio.2012.03.006.

Math5 defines the ganglion cell competence state in a subpopulation of retinal progenitor cells exiting the cell cycle

Joseph A. Brzezinski IV[1,2], **Lev Prasov**[1], and **Tom Glaser**[1]

[1]Departments of Human Genetics and Internal Medicine, University of Michigan Medical School, Ann Arbor, MI 48109

SUMMARY

The basic helix-loop-helix (bHLH) transcription factor *Math5* (*Atoh7*) is transiently expressed during early retinal histogenesis and is necessary for retinal ganglion cell (RGC) development. Using nucleoside pulse-chase experiments and clonal analysis, we determined that progenitor cells activate *Math5* during or after the terminal division, with progressively later onset as histogenesis proceeds. We have traced the lineage of *Math5+* cells using mouse BAC transgenes that express Cre recombinase under strict regulatory control. Quantitative analysis showed that *Math5*+ progenitors express equivalent levels of *Math5* and contribute to every major cell type in the adult retina, but are heavily skewed toward early fates. The Math5>Cre transgene labels 3% of cells in adult retina, including 55% of RGCs. Only 11% of *Math5*+ progenitors develop into RGCs; the majority become photoreceptors. The fate bias of the *Math5* cohort, inferred from the ratio of cone and rod births, changes over time, in parallel with the remaining neurogenic population. Comparable results were obtained using *Math5* mutant mice, except that ganglion cells were essentially absent, and late fates were overrepresented within the lineage. We identified *Math5*-independent RGC precursors in the earliest-born (embryonic day 11) retinal cohort, but these precursors require *Math5*-expressing cells for differentiation. *Math5* thus acts permissively to establish RGC competence within a subset of progenitors, but is not sufficient for fate specification. It does not autonomously promote or suppress the determination of non-RGC fates. These data are consistent with progressive and temporal restriction models for retinal neurogenesis, in which environmental factors influence the final histotypic choice.

Keywords

mouse; genetics; Cre recombinase; BAC transgenic; lineage; expression fate mapping; cell fate determination; retina; optic nerve; atonal; bHLH

INTRODUCTION

The seven major cell types in the vertebrate retina (rod and cone photoreceptors; amacrine, horizontal and bipolar interneurons; Müller glia; and ganglion cells) develop from a

Address correspondence to: Tom Glaser, MD PhD, 2047 BSRB, Box 2200, Department of Internal Medicine, University of Michigan Medical School, 109 Zina Pitcher Place, Ann Arbor, MI 48109-2200, tel: (734) 764-4580, fax: (734) 763-2162, lab: (734) 647-3255, tglaser@umich.edu.
[2]Current address: Department of Biological Structure, University of Washington, Seattle, WA 98105

common pool of progenitors (Turner and Cepko, 1987; Turner et al., 1990) that are established when the optic vesicles invaginate to form bilayered optic cups (Goldowitz et al., 1996). The inner layer of each optic cup consists of proliferative retinal progenitor cells (RPCs), which are arranged as a pseudostratified epithelium. These RPCs begin to permanently exit mitosis and differentiate around embryonic day 11 (E11) in the mouse. Retinal neurons and glia are fully formed by postnatal day 21 (P21) and are arranged in a highly ordered tri-laminated structure (Rodieck, 1998). The outer nuclear layer (ONL) consists of photoreceptors while the inner nuclear (INL) and ganglion cell (GCL) layers are populated by interneurons, glia and ganglion cells. The mechanism of cell fate determination – how these diverse cell types are generated from an initially homogeneous progenitor population – remains poorly understood.

Birthdating experiments, in which [^{3}H]-thymidine was used to mark the terminal S phase of progenitor cells, have established a characteristic order for the emergence of different retinal cell types during histogenesis (Carter-Dawson and LaVail, 1979; Rapaport et al., 2004; Sidman, 1961; Young, 1985). In all vertebrate species examined, retinal ganglion cells are the first-born neurons (Altshuler et al., 1991). In mammals, these are followed by horizontal cells, cones, amacrines, rods, bipolar cells and Müller glia, in descending birth order. There is considerable overlap in the distribution of birthdates among cell types, particularly for rod photoreceptors, which are born over an extended period (E13-P7 in mice) and are most abundant. Moreover, as a subclass, displaced amacrines, located in the mammalian GCL, are born earlier than amacrines in the INL (LaVail et al., 1991; Reese and Colello, 1992).

Lineage tracing experiments in rodents and frogs show that individual retinal progenitors are multipotent, giving rise to clones with heterogeneous cell type composition and size, and that the histogenic potential of the progenitor pool is gradually restricted over time (Holt et al., 1988; Turner and Cepko, 1987; Turner et al., 1990; Wetts and Fraser, 1988; Wong and Rapaport, 2009). The absence of a strict hierarchical relationship among cell types suggests that fate determination in the retina is a stochastic process (Gomes et al., 2011; Livesey and Cepko, 2001). The observation of discordant two-cell clones in rodent lineage marking studies indicates that at least some cell fate decisions occur during or after the terminal division, and may be subject to environmental influence (Turner and Cepko, 1987). Indeed, multiple extrinsic factors have been shown to alter the ratio of retinal cell types generated from progenitor pools (Altshuler et al., 1991; Ezzeddine et al., 1997; Fuhrmann et al., 1995; Yang, 2004; Young and Cepko, 2004).

Heterochronic mixing experiments, in which early and late retinal cells are co-cultured in unequal ratios, have shown that progenitors have a limited capacity to shift their fate forward or backward in sequence, and suggest that competence is fundamentally a cell-intrinsic property (Belliveau and Cepko, 1999; Rapaport et al., 2001; Reh, 1992; Watanabe and Raff, 1990). Likewise, single-cell dissociation studies have shown that the fates of retinal progenitors, including post-mitotic cells, change over time and are intrinsically programmed (Adler and Hatlee, 1989; Cayouette et al., 2003; Reh and Kljavin, 1989). Thus, it is likely that cell-intrinsic factors, expressed by progenitors in a prescribed temporal order, work in concert with extrinsic factors in the retinal microenvironment to guide cell fate decisions and ensure proper ratios of each cell type.

The basic helix-loop-helix (bHLH) transcription factor Math5 (Atoh7) was identified on the basis of its homology to *Drosophila* Atonal (Brown et al., 1998), which plays a critical role in the specification of R8 photoreceptors in the eye imaginal disc (Frankfort and Mardon, 2002; Hsiung and Moses, 2002; Jarman, 2000; Sun et al., 2003). The mouse *Math5* gene contains a single exon (Prasov et al., 2010) and is specifically expressed by progenitor cells during retinal histogenesis (Brown et al., 1998), similar to frog, chick, and zebrafish

orthologs (Kanekar et al., 1997; Liu et al., 2001; Masai, 2000). *Math5* mutant mice lack retinal ganglion cells (RGCs) and optic nerves (Brown et al., 2001; Wang et al., 2001) and their circadian rhythms are not photoentrained (Brzezinski et al., 2005; Wee et al., 2002). Retinal vascular development (Brzezinski et al., 2003) and electrophysiology (Brzezinski et al., 2005) are also disrupted in these mice. Finally, the relative abundance of other retinal cell types is altered, through a combination of cell autonomous and non-autonomous effects (Brzezinski et al., 2005; Le et al., 2006). RGC genesis similarly fails in *ath5* mutant (*lakritz)* zebrafish (Kay et al., 2001). In humans, *ATOH7* mutations cause optic nerve aplasia (Ghiasvand et al., 2011) and the *ATOH7* locus is a major determinant of normal variation in optic disc size, which reflects RGC number (Khor et al., 2011; Macgregor et al., 2010; Ramdas et al., 2010).

Math5 is likely to trigger a regulatory cascade for RGC development. Expression of the POU domain transcription factor *Brn3b* (*Pou4f2*) appears to be controlled by *Math5* in mice, similar to the orthologous circuit in chick and frog (Hutcheson and Vetter, 2001; Liu et al., 2001; Schneider et al., 2001; Wang et al., 2001). In turn, *Brn3b* and the homeodomain transcription factor *Isl1* form two regulatory nodes that are critical for RGC maturation (Erkman et al., 1996; Gan et al., 1996; Mu et al., 2004; Mu et al., 2008; Pan et al., 2008).

How does *Math5* regulate ganglion cell fate determination? In principle, *Math5* could act either as an *instructive* factor, irreversibly directing competent progenitors to differentiate into RGCs, or as a *permissive* factor, establishing an RGC competence state within a set of multipotent progenitors, only some of which develop into RGCs (Wessells, 1977). The Cre-lox recombination system provides a powerful tool to distinguish these mechanisms, by indelibly marking descendant cells. In a previous lineage analysis, a *Math5-Cre* knock-in allele was found to mark multiple retinal cell types, suggesting that Math5 acts permissively (Feng et al., 2010; Yang et al., 2003).

In this report, we extend these findings using a Math5>Cre BAC transgene in wild-type and *Math5* mutant mice. This approach, coupled with birthdating analysis, has allowed us to quantitatively assess the cell type distribution and unique fate trajectory of the Math5 lineage over time. Our results show *Math5* is expressed at equivalent levels in a subset of progenitors that are capable of forming all retinal cell types, with a frequency that decreases according to birth order. Although heavily weighted toward early fates, only 11% of these cells develop into RGCs and only 55% of RGCs descend from Math5+ progenitors. In the absence of *Math5* function, lineage-marked cells exhibit a similarly diverse range of fates but do not differentiate as RGCs, suggesting Math5 has both autonomous and non-autonomous roles in RGC development. Using cell cycle markers and nucleoside pulse-chase analysis, we show *Math5* expression is confined to progenitors during or after the terminal division, and does not control cell cycle exit. Finally, using retroviral clone analysis of explanted embryonic retinas, we demonstrate that *Math5*+ cells frequently arise in pairs from symmetric terminal divisions. Our results extend previous observations, but compel different conclusions. We provide new insights into *Math5* function, ganglion cell development, and the mechanism of retinal fate determination.

MATERIALS AND METHODS

Quantitative PCR

Eye tissue was collected from 8-12 CD-1 embryos or newborn mice at time-points between E10.5 and P1.5 and homogenized in Trizol reagent (Invitrogen, Carlsbad, CA). Total RNA was purified from pooled homogenates at each time-point. cDNA was synthesized using $d(N)_6$ primer and Superscript II reverse transcriptase (Invitrogen). Quantitative PCR was performed on cDNA using *Math5* and *Hprt* primers (Brown et al., 2001) with the iCycler iQ

system (Bio-Rad, Hercules, CA). Seven measurements were made for each cDNA pool. *Math5* RNA levels (critical threshold cycles) were normalized to *Hprt* as described (Livak and Schmittgen, 2001), and are reported relative to the mean P1.5 value.

Math5>Cre BAC transgenic mice

We replaced the *Math5* open reading frame on bacterial artificial chromosome (BAC) clone RP23-328P3 with a 2.0 kb nlsCre-actin pA cassette using a two-step *recA*-mediated recombination protocol in *E. coli* (Gong et al., 2002; Heintz, 2001). To target the BAC, which contains 110 kb 5′ and 103 kb 3′ genomic DNA flanking the *Math5* transcription unit (Prasov et al., 2010), we constructed a plasmid vector with short 5′ (A, 345 bp) and 3′ (B, 378 bp) homology arms flanking Cre-pA. These were amplified by PCR from UTR sequences of the solitary *Math5* exon (AF418923) and cloned into the *Sal*I and *Xho*I sites of p GSU-Cre (Cushman et al., 2000). The resulting A-Cre-B cassette was inserted into the *Xho*I site of shuttle plasmid pLD53 GFP10 as a 2.4 kb *Sac*I-*Xho*I fragment and verified by DNA sequencing. Shuttle plasmid pLD53 GFP10 was derived from pLD53.SC1 by partial *Spe*I digestion and insertion of a *Xho*I linker in place of the 3.5 kb EGFP fragment. We then targeted RP23-328P3 with the Math5>Cre shuttle vector pLD53 ACreB to obtain ampicillin- and chloramphenicol-resistant cointegrates (Gong et al., 2002). These were resolved by selection on TYE (tryptone-yeast extract) agarose plates with chloramphenicol and 10% (w/v) sucrose. Two recombinant Math5>Cre BAC clones were recovered and verified by PCR and pulsed-field gel electrophoresis (PFGE) Southern analysis.

Purified circular DNA from Math5>Cre BAC clone RP23-328P3-D1-68 was injected into fertilized (SJL/2 C57BL/6J) F_2 oocytes by the UM Transgenic Animal Core Facility. Nine transgenic founders were identified by Cre-specific and BAC vector-insert junctional PCRs. Transgene copy number was determined by Southern analysis, using an upstream *Math5* genomic probe that hybridizes equally well to 3.5 kb BAC and 6.5 kb mouse chromosomal *Eco*RI fragments. Transgene integrity was evaluated by Southern analysis following *Not*I digestion and PFGE. Transgenic offspring were genotyped using PCR primers within the Cre-pA cassette.

Math5>Cre mice (line 872 or 360) were crossed to Z/AP (JAX stock 003919, (Lobe et al., 1999) and R26*flox*GFP (JAX stock 004077, (Mao et al., 2001) reporter strains, which express membrane-tethered hPLAP (human placental alkaline phosphatase) or cytoplasmic GFP (green fluorescent protein), respectively, from ubiquitously active promoters, upon Cre-mediated excision of *floxed* upstream stop signals. Tissues from informative double transgenic progeny were collected from E11.5 to 15.5, on P0.5, and at 3-4 weeks of age. To trace lineage in the absence of *Math5* function, we crossed Z/AP; *Math5* −/− mice (*Atoh7*^{tm1Gla}, (Brown et al., 2001) to Math5>Cre (line 360); *Math5* +/− mice and compared the patterns of hPLAP staining in 3-4 week-old double transgenic mutants and heterozygous controls.

Histology

Embryonic and adult eyes were fixed overnight in 4% paraformaldehyde (PFA) at 4°C, cryoprotected in phosphate-buffered saline (PBS) with 10 to 30% sucrose, frozen in OCT compound (Tissue-Tek, Torrance, CA), and cryosectioned at 5-10 m. For Brn3b (Pou4f2) and cyclin D1 epitopes, fixation was 30 min at room temperature in 2% PFA. For immunodetection, cryosections were blocked for 4 hrs at room temperature in PBTx (0.1 M $NaPO_4$ pH 7.3 0.5% Triton X-100) with 10% normal donkey serum (NDS) and 1% bovine serum albumin (BSA). Sections were incubated overnight at 4 C with primary antisera or biotinylated PNA (peanut agglutinin) lectin diluted in PBTx with 3% NDS and 1% BSA. For fluorescence detection, sections were incubated for 2 hrs at room temperature with

appropriate secondary antibodies or streptavidin conjugates (Jackson Immunoresearch, West Grove, PA). Nuclei were identified using 100 ng/mL 4′,6-diamidino-2-phenylindole (DAPI). For chromogenic detection, sections were stained using the avidin-biotin complex method (Vector, Burlingame, CA) with HRP (horeseradish peroxidase)-conjugated streptavidin and diaminobenzidine (Brown et al., 2001).

The primary antibodies were mouse anti-β-galactosidase (βgal, monoclonal 40-1A, 1:500, DSHB, Iowa City, IA); rabbit anti-βgal (1:5000, ICN Cappel, Aurora, OH); rat anti-βgal (1:500, (Saul et al., 2008)); rat anti-BrdU (monoclonal BU1/75, 1:100, Harlan Seralab, Indianapolis, IN); mouse anti-calbindin (monoclonal CB-955, 1:500, Sigma, St. Louis, MO); mouse anti-Cre (monoclonal 7.23, 1:300, Covance, Princeton, NJ); mouse anti-cyclinD1 (sc8396, 1:100, Santa Cruz Biotechology, Santa Cruz, CA); rabbit anti-GFP (1:5000, Upstate, Lake Placid, NY); chicken anti-GFP (1:2000, Abcam, Cambridge, MA); mouse anti-hPLAP (monoclonal 8B6, 1:250, Sigma); mouse anti-Ki67 (monoclonal MM1, 1:25, Novocastra, Newcastle, UK); rabbit anti-mGluR2/3 (1:200, Chemicon); goat anti-Neurod1 (sc1084, 1:50, Santa Cruz); rabbit anti-phosphohistone H3 (1:400, Upstate, Lake Placid, NY); rabbit anti-rhodamine (1:500, Invitrogen). Biotinylated PNA (Vector) was used at 1:250.

For simultaneous detection of BrdU (5-bromo-2-deoxyuridine) and other markers, cryosections were fully stained with primary antibodies and lectins, and fluorescent secondary reagents. Sections were then treated with 2.4 N HCl in PBTx for 60-75 min at room temperature, washed, and immunostained for BrdU. EdU (5-ethynyl-2-deoxyuridine) was detected using an azide-alkyne cycloaddition reaction (Buck et al., 2008) and commercial reagents (Click-iT-647, Invitrogen) after immunostaining. For EdU and BrdU co-labeling, BrdU immunostaining was performed as the final step. For Ki67 immunostaining, sections were unmasked before the blocking step by heating to 95°C for 10 min in 0.01 M citric acid.

For chromogenic detection of hPLAP activity in retina, 5-10 μm cryosections were heat-treated for 30 min in PBS with 2 mM $MgCl_2$ at 70 C and stained with 5-bromo-4-chloro-3-indolyl phosphate (BCIP) and nitroblue tetrazolium (NBT) substrates (Roche, Indianapolis, IN) for 1.5 hrs (Lobe et al., 1999). To detect hPLAP activity in the brain, adult tissues from transgenic animals were immersion-fixed in 4% PFA, 2 mM $MgCl_2$ at 4 C overnight, heat-treated for 45 min in PBS with 2 mM $MgCl_2$ at 70 C, and embedded in 3% agarose. Thick coronal vibratome sections (250 m) were stained for hPLAP activity as floating slices in 24-well plates in AP buffer containing 0.01% Na deoxycholate, 0.02% NP-40, 2 mM levamisole, and BCIP/NBT substrate (Roche), for 5-6 hrs at room temperature. Sections were washed in PBS containing 20 mM EDTA, dehydrated through a graded ethanol series, cleared with BABB (1:2 benzyl alcohol: benzyl benzoate) and mounted in Permount (Fisher Scientific, Pittsburgh, PA). Chromogenic detection of -galactosidase (gal) activity with 5-bromo-4-chloro-3-indolyl-β-D-galactopyranoside (Xgal) substrate and *in situ* RNA hybridization were performed as described (Brown et al., 2001).

Images were obtained using a Nikon Eclipse E800 epifluorescence microscope and a SPOT digital camera. Low power images of brain sections were captured using a Zeiss Axioimager Z1 microscope with 5X objective. Confocal images were collected using a Noran OZ Laser Scanning Confocal assembly microscope or Zeiss LSM510 Meta imaging system.

Labeling RGCs by retrograde axonal tracing

To unequivocally identify all RGCs, we performed retrograde axon labeling with a rhodamine dextran tracer (Farah and Easter, 2005; Rachel et al., 2002). Eyes from adult Math5>Cre; R26*flox*GFP mice were rapidly immersed in artificial cerebral spinal fluid

(aCSF) (von Bohlen und Halbach, 1999). The optic nerves were transected within 1 mm of the sclerae and pressed against 4 mm cubes of surgifoam (Ethicon, Somerville, NJ) saturated with 3% L-α-lysophosphatidyl choline (LPC, Sigma) and lysine-fixable tetramethyl rhodamine dextran 3,000 MW powder (Molecular Probes, Eugene, OR). Each eye and surgifoam cube was sealed with 1% agarose and incubated in aerated aCSF for 1 hr at room temperature. The eyes were then incubated overnight in fresh aCSF without surgifoam, fixed in 4% PFA for 4-6 hrs at room temperature, cryoprotected in PBS with 10 to 30% sucrose, and frozen in OCT. For P1 mice, the same retrograde labeling procedure was followed, except that eyes were immersed in Hank's balanced salt solution containing calcium, magnesium and 1 mM glucose (Gerfen et al., 2001). After labeling, eyes were fixed in 4% PFA for 1 hr. The dissected retinas were post-fixed for 3 hrs, immunostained and flatmounted for imaging.

Math5 cell cycle analysis

Retinas from *Math5* +/− and *Math5* −/− embryos (carrying the *lacZ* knock-in allele) were co-labeled for gal, BrdU or EdU (S phase), phosphohistone H3 (M phase (Bradbury, 1992)), cyclinD1 (G1 and early S phases (Yang et al., 2006)), and Ki67 (S, G2, M and late G1 phases, (Key et al., 1993)). To label cells in S phase, pregnant dams were given a single intraperitoneal injection of EdU (6.7 μg/g of body mass) or BrdU (100 μg/g) 30-60 min prior to harvest. To test whether *Math5*+ progenitors re-enter the cell cycle, lineage-marked Math5>Cre embryos carrying Z/AP or R26*flox*GFP reporters were similarly pulsed with BrdU or EdU and their retinas co-stained for hPLAP, GFP or Cre and cell cycle markers.

Quantitative lineage analysis

Math5+ descendants were revealed by hPLAP or GFP immunolabeling in 200 adult retinal sections. Cell types were identified by laminar position, characteristic morphology, expression of diagnostic markers, and retrograde axon tracing. Lineage-marked cones were distinguished from rods by co-labeling with anti-hPLAP and PNA lectin (Blanks and Johnson, 1983). Because strong hPLAP staining in cone pedicles obscured horizontal cell bodies, we identified these cells using the R26*flox*GFP reporter and calbindin immunostaining (Peichl and Gonzalez-Soriano, 1993). Horizontal cells were surveyed in 58 sections from Math5>Cre; R26*flox*GFP mice (8 eyes). GFP-positive rhodamine-dextran labeled RGCs and DAPI-labeled nuclei (RGCs + displaced amacrines) were counted within the GCL in 33 fields (200X magnification) representing 8 Math5>Cre; R26*flox*GFP adult eyes. For P1 counts, the fraction of lineage-labeled RGCs was determined in retinal flatmounts from 3 eyes. The fraction of each cell type descending from *Math5+* progenitors, and the fraction of *Math5+* progenitors giving rise to each cell type, were calculated based on detailed retinal cell counts reported for adult C57BL/6J mice (Jeon et al., 1998). For lineage tracing in the absence of *Math5* gene function, labeled cells were counted in 23 fields (200X magnification) representing 6 adult eyes.

Dual reporter concordance

To assess Math5>Cre efficiency and heterogeneity among *Math5+* progenitors, we crossed Math5>Cre; Z/AP mice to homozygous R26*flox*GFP mice. Retinal sections from 3-4 week-old triple transgenic offspring (Math5>Cre; Z/AP; R26*flox*GFP) were immunostained for GFP and hPLAP. Single- and double-labeled cones, rods, amacrines and GCL neurons were counted in 18 fields (200X magnification) representing 4 eyes. To calculate concordance, we divided the number of double-labeled cells by the total number of labeled cells. Concordance was evaluated statistically using Cohen's κ test (Cohen, 1960).

Birthdating and window labeling studies

To identify *Math5* descendants exiting mitosis before P0, we performed a cumulative BrdU labeling experiment (Miller and Nowakowski, 1988). Pregnant dams carrying Math5>Cre; Z/AP embryos were given a single BrdU injection (100 g/g body mass) on day E10.5 and provided with drinking water containing 500 g/mL BrdU and 1% sucrose (pH 7.0) until birth (Mayer et al., 2000). To maximize labeling efficiency, water bottles were protected from light and replaced daily. Retinal sections from 3-week-old offspring were immunostained for BrdU and hPLAP.

To monitor how the fates of *Math5+* progenitors exiting mitosis change during development, we performed birthdating (pulse-labeling) experiments. Pregnant dams carrying Math5>Cre; Z/AP embryos were given a single BrdU injection (as above) on day E14.5, E15.5, E16.5 or E17.5 of development. Eyes from 3-4 week-old mice were stained with BrdU and hPLAP antibodies, and PNA lectin. The total number of cones (PNA+) and the number of hPLAP+ and/or BrdU+ photoreceptors were counted in 14 central retinal fields (200X magnification), corresponding to 3 eyes for each time-point. For birthdating lineage-marked photoreceptors in the absence of *Math5* function, we followed the same protocol as above. We immunostained Math5>Cre; R26*flox*GFP; *Math5* −/− retinas for BrdU and GFP, and counted ≥7 fields (200X magnification) from 2-4 eyes for each time-point. The fraction of lineage-marked and birthdated cones was calculated directly from cell counts. The fraction of labeled rods was estimated using a 35.2 rod-to-cone ratio for wild-type mice, based on C57BL/6 data (Jeon et al., 1998), and a 12.1 ratio for *Math5* mutants (SEM = 0.8 based on n = 5 animals, 71 fields at 200X magnification).

To determine the contribution of *Math5+* cells to the early-born (EB) cohort of neurons, we performed pulse- and window-labeling experiments at the onset of neurogenesis. For pulse-labeling, gravid dams carrying Math5>Cre; R26*flox*GFP embryos were given a single injection of EdU at day E11, and eyes from the resulting pups were harvested at P1. Whole retinas were stained for GFP and EdU, flatmounted, and imaged as confocal Z-stacks through the ganglion cell layer. The fraction of early-born cells in the *Math5* lineage (EdU+ GFP+ / EdU+) was determined from 4 eyes representing 4 mice.

For window labeling (Repka and Adler, 1992), pregnant dams carrying *Math5* +/− and −/− embryos were given EdU on day E11, as a single injection or two injections 12 hrs apart. No difference was apparent in the extent of EdU labeling between these schedules. Dams were then given a single injection of BrdU on E12 and provided with BrdU in the drinking water until harvest at E12.5. Early-born cells (EdU+ BrdU−) were counted from 3-4 embryos of each genotype, representing 1-3 litters, and scored for βgal or Brn3b immunoreactivity. Statistical error is reported as the binomial standard deviation. Labeled fractions were compared using Fisher's exact test (Fisher, 1925).

Retinal explants and clonal analysis

Retinal explant culture and retroviral infections were performed using established methods, which favor RGC survival (Hatakeyama and Kageyama, 2002; Wang et al., 2002). *Math5 lacZ*/+ retinas were dissected from E12.5 or E13.5 eyes, removing sclerae, pigmented epithelium (RPE) and lens tissue, and were flattened onto 5 mm Nucleopore polycarbonate membranes (0.4 μm pore size, GE Healthcare, Piscataway, NJ). These explants were placed on Transwell inserts (Corning) in 2-cm dishes containing neurobasal media (Invitrogen) with 1X B27 and N2 supplements, glutamine (0.4 mM), BDNF (50 ng/mL, Peprotech, Rocky Hill, NJ), CNTF (10 ng/mL, Peprotech), penicillin (50 U/mL), streptomycin (50 μg/mL), and gentamicin (0.5 μg/mL), and cultured at the gas-media interface at 37 C and 5% CO_2.

MIG retroviral stocks (Van Parijs et al., 1999) were generated by transfecting MSCV-IRES-GFP plasmid DNA into the Phoenix ecotropic packaging cell line (Pear, 2001; Swift et al., 2001) and titered on NIH3T3 fibroblasts. Filtered viral preparations (~8×10^5 colony-forming units/mL) containing polybrene (hexadimethrine bromide, 0.8 μg/mL, Sigma Aldrich, St. Louis, MO) were added directly to the explant surface in one drop (25 μL) to infect mitotic cells. After 2 days *in vitro* (DIV), half of the media was replaced with fresh media. After 3 DIV, explants were fixed for 30 min in 4% PFA, cryoprotected in 30% sucrose, and frozen in OCT. Thick (30 μm) sections were immunostained for βgal and GFP. For each time-point, the size and composition of clones was determined by 3-dimensional analysis of confocal Z-stacks. Clones were defined as clusters of GFP+ cells directly apposed to each other (within 2-3 μm) and separated by at least 4 cell bodies from any other GFP+ cells. Only clones containing at least two GFP+ cells and one βgal+ cell were scored. Previous studies have shown that the average progenitor cell cycle length is 14-16 hrs at this stage (Alexiades and Cepko, 1996; Sinitsina, 1971), permitting 4-5 divisions during the 72 hr culture period. Accordingly, the largest clones in each set of explants contained 8-16 cells, reflecting a minimum of 3-4 divisions *in vitro*.

RESULTS

Math5 is transiently expressed by early retinal progenitors during or after their terminal cell cycle

As a first step to determine the mechanism of *Math5* action, we defined the timing of *Math5* expression during retinal development by quantitative PCR (Fig. 1A). *Math5* mRNA increases rapidly at E11, peaks between E12.5 and E14.5, and declines gradually after E14.5. This temporal profile is consistent with RNA *in situ* hybridization data (Brown et al., 1998) and closely resembles birthdating curves for RGCs (Drager, 1985; Young, 1985). These data suggest *Math5* acts transiently during early retinal neurogenesis.

The cellular distribution of *Math5* mRNA and *Math5-lacZ* activity across the retinal epithelium (Brown et al., 2001) is consistent with *Math5* transcription in actively proliferating and/or postmitotic cells. Both patterns have been reported for different bHLH genes during neurogenesis (Kageyama and Nakanishi, 1997). Indeed, the closely related gene *Math1* is expressed in mitotic cells in the developing cerebellum (Helms et al., 2000) and in postmitotic cells in the inner ear (Chen et al., 2002). In frog, zebrafish and chick retinas, orthologous *Ath5* genes are expressed in progenitors during their last cell division (Matter-Sadzinski et al., 2001; Perron et al., 1998; Poggi et al., 2005).

To determine the onset of *Math5* expression in individual mouse retinal progenitors, we immunostained E13.5, E15.5, and E16.0 eyes from *Math5* +/− (*lacZ*/+) and/or *Math5* −/− (*lacZ/lacZ*) embryos for β-galactosidase (βgal), the cell cycle marker phosphohistone H3 (PH3, M phase), cyclin D1 (cycD1, G1/early S phase) (Yang et al., 2006) or Ki67 (late G1, S and M phase), and the thymidine analog EdU or BrdU (S phase) following a 30-60 minute pulse *in vivo*. After the EdU pulse, a small fraction of S phase progenitor cells enter G2 and are detected as EdU+ cycD1-. In contrast, cells remaining in S phase are EdU+ cycD1+. After careful 3-dimensional analysis of confocal Z-stack images, we observed a small number of βgal-expressing cells that had incorporated EdU at E13.5 (18 of 517 = 3.5 0.6% SD) for $n = 3$ sections, Fig. 1B). These βgal+ cells were exclusively cycD1− (0 of 517, upper limit 95% CI = 0.6%), indicating that *Math5* is expressed after G1 phase at E13.5. Accordingly, βgal+ PH3+ cells (M phase) were observed at E13.5 (Fig. 1D, (Le et al., 2006)). In contrast, in E15.5 and E16.0 embryos (Fig. 1C,E,G), few or no cells co-expressed βgal and cell cycle markers EdU, BrdU, cyclinD1, or PH3. The dynamics of *Math5* expression thus change during development. At early stages (<E14), some progenitors initiate *Math5* expression during the last cell cycle, whereas at later stages (>E15),

progenitors express *Math5* only after terminal mitosis. Similar results were observed in E15.5 *Math5* knockout embryos (Fig. 1F,H) (Le et al., 2006), demonstrating that βgal+ mutant cells do not re-enter the cell cycle. In *Math5* +/− and −/− mice, βgal+ cells span the entire retinal thickness (arrowheads in Fig. 1G,H), suggesting that radial processes associated with interkinetic nuclear migration may persist transiently, potentially directing the migration of early post-mitotic cells to their final laminar positions (Barnstable et al., 1985; McLoon and Barnes, 1989; Snow and Robson, 1994; Watanabe et al., 1991).

Math5>Cre lineage marking system

We designed an expression fate-mapping system to permanently mark lineal descendants of *Math5*-expressing progenitors and thereby define the range of fates acquired by these cells. The system has two components – transgenic mice expressing Cre recombinase under strict *Math5* regulatory control (Math5>Cre) and reporter mice (Z/AP or R26*flox*GFP) that express a histochemical marker (hPLAP or GFP) wherever Cre excises a *loxP*-flanked stop signal.

The Math5>Cre recombinant BAC (Fig. 2A,B) includes all likely *Math5* regulatory elements (Ghiasvand et al., 2011; Hutcheson et al., 2005). We generated nine Math5>Cre founders, each of which contains 1-5 copies of the BAC transgene (Suppl. Fig. 1A). Five lines were tested using Z/AP reporter mice, which conditionally express hPLAP under control of the ubiquitous CAG promoter (Lobe et al., 1999). Each line gave a similar staining pattern, which is consistent with the spatiotemporal expression of *Math5* mRNA (not shown). All subsequent experiments were performed with lines 872 and 360, which contain full-length transgene insertions, as determined by diagnostic PCR, Southern and PFGE analysis (Suppl. Fig. 1B).

From the onset of retinal neurogenesis (E11), *Math5* mRNA is expressed in cells near the ventricular (sclerad) neuroepithelial surface, where the majority of progenitors undergo mitosis (Brown et al., 1998). In *Math5-lacZ* knock-in mice, -galactosidase protein is expressed in a similar pattern but perdures (Echelard et al., 1994) in the differentiating descendants of these cells, including RGCs (Brown et al., 2001). In double transgenic Math5>Cre; Z/AP embryos, the alkaline phosphatase (hPLAP) marker first appeared at E12.5 in differentiating RGCs and the developing optic nerve (Fig. 2D), whereas no hPLAP was detected in control embryos carrying Z/AP alone (Fig. 2C). At later developmental stages, some other cell types were labeled with hPLAP (e.g. photoreceptors at P0.5 in Fig. 2D, arrowhead). As expected, hPLAP was only detected in the adult retina and brain, in known *Math5* RNA expression domains. In the central nervous system, the hPLAP reporter marks neurons in the auditory hindbrain and cerebellum (Saul et al., 2008) and reveals all known RGC projections (Rodieck, 1998; Simpson, 1984), including those extending to the superior colliculi, lateral geniculate bodies, suprachiasmatic nuclei, and the accessory optic tracts (Fig. 2E).

In the E15.5 retina, a comparison of the spatial and temporal patterns for *Math5* mRNA, *Math5-lacZ* and hPLAP (Fig. 2F) is consistent with a direct role for *Math5* in RGC development and highlights the inherent time delay associated with Cre protein synthesis, excisional activation of the Z/AP reporter, and expression of the hPLAP enzyme (Nagy, 2000). Considering the dynamics of retinal interkinetic nuclear migration (Baye and Link, 2008), these results suggest there is a burst of *Math5* expression in progenitors exiting the cell cycle. If *Math5* is exclusively made during the last division, lineage-marked cells should never re-enter S phase. To test this prediction, we analyzed E13.5 Math5>Cre; R26*flox*GFP and E15.5 Math5>Cre; Z/AP embryos exposed to EdU or BrdU for 1 hr (Fig. 2G,H). In E13.5 embryos after a 30 min chase, some Cre+ EdU+ cells were present (33 of 394 Cre+ cells = 8.4 0.4% SD for $n = 3$ sections) and these were restricted to the fresh neurogenic

subset (33 of 223 Cre+ GFP-cells = 14.8 1.4% SD). No GFP+ EdU+ cells were observed in the same sections (0 of 309 GFP+ cells, upper limit 95% CI = 0.9%), due to the delay in the Cre-lox system (Fig. 2G). Likewise, in E15.5 embryos, there was no overlap between hPLAP activity and any cell cycle marker (Fig. 2H). Together, these results strongly suggest that *Math5* is expressed transiently during or shortly after the terminal cell division. *Math5* lineage cells do not re-enter the cell cycle.

Quantitative *Math5* lineage analysis

To reveal the fates of *Math5+* progenitors, we crossed Math5>Cre mice to Z/AP and R26*flox*GFP reporter strains and examined mature retinas of 3-4 week old offspring. We observed hPLAP+ cells distributed evenly across the central and peripheral retinas of Math5>Cre; Z/AP mice, but staining was absent in littermates carrying the Z/AP transgene alone (Fig. 3A,B). Because hPLAP protein is membrane-tethered, we could identify most retinal cell types by morphology and laminar position. As expected, RGCs were abundantly labeled. However, we also observed significant staining among rods, cones, horizontal and amacrine cells (Fig. 3A,C,D). The inner plexiform layer (IPL) was intensely labeled due to hPLAP localization in RGC and amacrine dendrites. A thorough survey revealed rare hPLAP+ Müller glia and bipolar cells (Fig. 3C). Importantly, no labeling was observed in retinal cell types that have a separate developmental origin, such as vascular endothelial cells, pericytes, microglia and astrocytes, or in any other parts of the eye, including the anterior chamber and RPE.

To systematically measure the fraction of lineage-marked retinal cells in each class, we co-stained sections for hPLAP or GFP reporters and cell type-specific markers. Equivalent results were obtained using Z/AP and R26*flox*GFP reporters (see below) and different Math5>Cre lines (data not shown). However, the intensity of expression varied among cell types. Z/AP is strongly expressed in photoreceptors via the CAG promoter, whereas R26*flox*GFP is weakly expressed by photoreceptors but strongly expressed by other cell types. Consequently, we used Z/AP to count hPLAP+ and hPLAP-cones (arrows in Fig. 3D), and hPLAP+ rods (arrowheads in Fig. 3D) in the outer nuclear layer (ONL), and PNA lectin to distinguish cones from rods (Blanks and Johnson, 1983). We then counted hPLAP+ bipolar cells and Müller glia (Fig. 3C) in the inner nuclear layer (INL) of the same sections. The labeled fraction was calculated for each cell type using reference data for cell populations in the adult mouse retina (Jeon et al., 1998). This fraction ranged from 31% for cones to 1% for rods, and <0.1% for bipolar cells and Müller glia (Table 1).

To evaluate horizontal, ganglion and amacrine cell types, we used the R26*flox*GFP reporter, which co-localizes with cell type-specific markers in the perinuclear cytoplasm. We identified horizontal cells by calbindin immunostaining (Peichl and Gonzalez-Soriano, 1994) and their position at the outer edge of the INL (Fig. 3E). Twenty-nine percent of horizontals were GFP+ (Table 1). This value is significantly lower than that reported by Yang et al. (2003), but consistent with horizontal cell labeling data of Feng et al. (2010, *cf.* Suppl. Fig. 3E) obtained using a *Math5-Cre* knock-in allele. RGCs were distinguished from displaced amacrine cells (Hayden et al., 1980; Perry and Walker, 1980) by retrograde rhodamine-dextran tracing of optic nerve axons. Forty-three percent of neurons in the ganglion cell layer (GCL) were labeled with rhodamine in this experiment (arrows, Fig. 3F), in close accord with previous data (Jeon et al., 1998). All other cells in the GCL were scored as displaced amacrines (arrowheads, Fig. 3F). The frequency of GFP labeling in the adult retina was 55% for ganglion cells, 28% for displaced amacrines, and 9% for INL amacrines (Table 1). To evaluate the *Math5* lineage fraction prior to the normal period of RGC culling (Galli-Resta and Ensini, 1996), we performed a similar analysis in early postnatal retinas, limited to the GCL (Fig. 3G). The fraction of GFP+ ganglion cells in P1 retinas (53 ± 1%, *n*

= 3, 948/1777 cells) was similar to that observed in the adult (55 ± 2%, Table 1, Fisher's exact test $P = 0.3$).

A clear pattern emerges from these data. First, *Math5+* progenitors have the potential to develop into all seven major retinal cell types. Second, the distribution of *Math5+* descendents differs from the retina as a whole (Fig. 3I, χ^2 test with $df = 7$, $P < 0.0001$). Third, the labeling fraction of each cell type (Table 1) decreases according to the birth order (Carter-Dawson and LaVail, 1979; Rapaport et al., 2004; Sidman, 1961; Young, 1985). Early-born cell types – RGCs, cones, horizontal cells and displaced amacrines – frequently descend from *Math5+* progenitors, whereas late-born bipolar and Müller glial cells rarely derive from *Math5+* progenitors. INL amacrines are born during the middle phase of retinal development, prior to the peak of rod births, and these cell types have an intermediate labeling fraction. We estimate that 3% of adult retinal cells descend from *Math5+* progenitors (Table 1). Fourth, only one in nine *Math5+* descendants is a ganglion cell (11%). Because RGCs represent ~0.5% of neuroretinal cells in adult mice (Jeon et al., 1998) and *Math5* status does not affect RGC survival between P1 and adulthood, *Math5* descendants are 50-fold more likely on average to develop as RGCs than the remaining neuroretinal population (approx. 1 in 500). Fifth, 45% of ganglion cells are not marked by the Math5>Cre transgene, suggesting the possibility of a substantial *Math5*-independent RGC subpopulation. Although the fraction of GCL neurons labeled by Math5>Cre (40%, Table I) approximates the RGC fraction (43%), this value includes both RGC (24%) and displaced amacrine cell types (16%).

The fate of *Math5* mutant cells

In mutant mice, the *Math5* transcription unit is active, expressing *lacZ* mRNA, but lineage-marked progenitors are blocked from developing as RGCs. To determine the fates of these cells, we examined retinas from adult *Math5* −/− mice carrying Z/AP and Math5>Cre transgenes (Fig. 3H). The extent of hPLAP labeling in the mutant retina was roughly similar to wild-type (Fig. 3A). However, the fate profile within the Math5 lineage was different (χ^2 test with $df = 7$, $P < 0.0001$). First, RGCs were absent, as expected, decreasing the amount of IPL staining. Second, there was an obvious increase in 'late-born' cell types among the hPLAP+ neurons (Suppl. Table 1). For example, rod photoreceptors increase from 32% to 40% of the Math5 lineage. Labeled bipolar cells and Müller glia were visible in most low power fields (200X magnification) of mutant mice, but were difficult to find in wild-type Math5>Cre; Z/AP retinas (Table 1), consistent with results observed by (Feng et al., 2010). This effect is more striking if one considers that the total number of rods, bipolar cells and Müller glia are decreased in *Math5* mutants (Brown et al., 2001; Brzezinski et al., 2005). In *Math5* mutant mice, the cohort of progenitors expressing Math5>Cre does not differentiate into RGCs, but retains competence to develop into any of the remaining principal cell types.

Math5+ progenitors have equivalent Cre activity

Only a small fraction (11%) of the *Math5* lineage develops into RGCs. In principle, the *Math5+* population may be heterogeneous, such that one group of progenitors expresses high levels of Math5>Cre and develops as RGCs, while a second group expresses low levels of Math5>Cre and adopts other fates (Fig. 4A). In this model, the low-level multi-lineage Math5>Cre expression could represent 'priming' (Hu et al., 1997) of the *Math5* gene, or leaky transgene expression, an 'over-reporting' artifact that is not biologically meaningful (Dymecki et al., 2002). Alternatively, all *Math5+* progenitors may express equivalent levels of Math5>Cre (Fig. 4B), consistent with a permissive role for *Math5* in retinal development.

To test these alternatives, we examined retinas from triple transgenic (Math5>Cre; Z/AP; R26*flox*GFP) adult mice, using the concordance of hPLAP and GFP labeling in *Math5*

descendants as an indirect measure of Cre activity (Fig. 4C). In this experiment, we assume that the probability of reporter activation in a particular cell depends on the concentration and stability of intracellular Cre protein, and that neither reporter is saturated at the Cre levels under investigation. Progenitors with strong Cre expression are expected to activate both reporters, while progenitors with weak Cre expression may randomly activate one reporter, Z/AP or R26*flox*GFP, at a low frequency (Fig. 4A,B). If these events occur independently with equal probability (ρ), then the joint probability of observing both reporters in a single cell (expected concordance) should equal $\rho^2/(2\rho-\rho^2)$, where ρ^2 is the fraction of cells that activate both reporters and $2\rho-\rho^2$ is the fraction of cells that activate at least one reporter. The observed concordance was uniformly high (~80%) for rods, cones, INL amacrines and GCL neurons, and much greater than expected by chance (Cohen's κ > 0.7, Fig. 4D, Suppl. Table 2). Thus, the labeling of non-RGC cell types cannot be attributed to differential or leaky Math5>Cre expression.

The fate of the *Math5+* progenitor population changes over time

The discovery that some rods, bipolars and Müller glia descend from Math5>Cre progenitors (Table 1) is somewhat surprising because the vast majority of these cell types undergo terminal mitosis (Rapaport et al., 2004; Young, 1985) after the temporal envelope of *Math5* mRNA expression (Fig. 1A). To explain these findings, we performed a cumulative labeling experiment, in which Math5>Cre; Z/AP embryos were continuously exposed to BrdU from E10.5 until P0 and analyzed at P21. Retinal progenitors that exit mitosis before P0 should be heavily BrdU-labeled, whereas those that continue to divide after P0 should be weakly labeled. We found that essentially all hPLAP+ cells in the central retina were heavily labeled with BrdU (98.8%), including rods (arrowheads in Fig. 5A), cones (arrows in Fig. 5A), and INL and GCL neurons (Suppl. Table 3). Therefore, *Math5+* rods, bipolars and Müller glia are born at the 'leading edge' of birthdating curves for these 'late' cell types.

The fate profile of neurogenic cells emerging from the RPC population is known to change over time, in response to intrinsic factors and environmental signals (Livesey and Cepko, 2001; Rapaport et al., 2004; Young, 1985). This can occur through alterations in the fate bias of individual cells or the composition of the RPC pool (heterogeneity). In principle, the *Math5+* cohort may behave similarly. The fate profile of these cells may be intrinsically programmed, or it may vary depending on the time that an individual RPC exits mitosis and initiates *Math5* transcription. To test these alternatives, we compared the fates of *Math5+* progenitors born on different days. Math5>Cre; Z/AP embryos were exposed to a pulse of BrdU on E14.5, E15.5, E16.5 or E17.5 and their adult retinas were examined by hPLAP, PNA, and BrdU staining (Fig. 5B). A variety of lineage-marked cell types were born on each of these days, including RGCs, rods, cones, amacrines and horizontal cells, as well as rare 'late' cell types (arrowhead in Fig. 5B). For quantitative analysis, we focused on photoreceptors, which are relatively numerous and could be directly compared within the ONL. At each time-point, we determined the fraction of hPLAP+ and heavily BrdU+ rods and cones in the central retina (arrows in Fig. 5B, Suppl. Table 4). The fraction of photoreceptors (rods plus cones) that were derived from *Math5+* progenitors decreased between E14.5 and E17.5, from 20.6% to 4.3% (Suppl. Fig. 2, Suppl. Table 4), in parallel with the decrease in the total number of *Math5+* cells.

The fate of the *Math5+* cell population also changed significantly between E14.5 and E17.5, together with the retina as a whole. *Math5+* cells born on E14.5 were >2 times as likely to develop into cones as compared to rods (136 vs. 64), whereas those born on E17.5 were >60 times as likely to develop into rods as compared to cones (122 vs. 2, Suppl. Table 4). The fates of progenitors inside and outside the *Math5* lineage shifted in parallel, as shown by plots of the cone-to-rod ratio (Fig. 5C), derived from birthdating curves (Suppl. Fig. 2). This

shift is primarily determined by the overall decrease in cone births during this interval. *Math5+* cells appear to follow the same fate trajectory as other progenitors. However, the ratio curves are displaced by one-half day. In comparison to other neurogenic cells (hPLAP −) exiting mitosis on the same day in the same retinal environment, Math5+ progenitors (hPLAP+) were three times more likely to develop into cones. Surprisingly, similar results were obtained in the absence of *Math5* function, in mutant embryos carrying R26*flox*GFP and Math5>Cre transgenes (Fig. 5D).

These findings support three conclusions. First, the fate profile of *Math5+* cells changes over time, similar to that of other retinal progenitors. Second, the fate bias of *Math5*+ cells extends beyond RGC specification, influencing the choice among alternative fates (e.g. cone vs. rod). Third, the bias among alternative fates is independent of *Math5* action, suggesting that upstream or parallel factors are responsible.

Math5 expression in early-born retinal cells

Because *Math5* expression is closely correlated with the onset of retinal neurogenesis (~E11.5) (Hufnagel et al., 2010) and is essential for specification of the earliest born cell type, RGCs (Brown et al., 2001; Wang et al., 2001), we expected that most or all early-born retinal cells would express *Math5* and adopt RGC fates. To test this hypothesis, we performed a series of window-labeling experiments. Embryos were sequentially exposed to EdU at E11 and BrdU at E12 (Fig. 6A). In this paradigm, cells incorporate EdU if they are in S phase at E11. Because the average cycle length at this stage is less than 24 hrs (Sinitsina, 1971), EdU+ BrdU+ cells scored at E12.5 are interpreted as RPCs that underwent one additional division (and S phase). In contrast, EdU+ BrdU-cells define the early-born (EB) cohort. These cells were in S phase at E11, but exited the cell cycle before E12.5.

To evaluate RGCs within the EB cohort, we counted the fraction of EdU+ BrdU-cells that were Brn3b+ (RGCs) in *Math5* heterozygous and mutant mice (Fig. 6B). In *Math5* +/− embryos, 75% of the EB cohort expressed Brn3b, confirming that RGCs are the predominant first-born cell type (Farah and Easter, 2005; Rachel et al., 2002). The abundance of EdU+ BrdU-cells was similar in *Math5* −/− and +/− embryos (5.7 vs. 7.1 per 0.001 mm^2 field, respectively) and comparable to previous birthdating results (Le et al., 2006). However, in *Math*5 mutant embryos, only 6% EdU+ BrdU-cells expressed Brn3b. This was expected from the deficiency of RGCs in these mice, and confirms that the loss of RGCs is an early event. We next determined the fraction of EdU+ BrdU-cells that expressed *Math5*, using the *lacZ* allele (βgal) as a short-term lineage tracer (Wang et al., 1999). Surprisingly, only 20% of EdU+ BrdU-cells were βgal+, in both *Math5* +/− and *Math5* −/− mice (Fig. 6C). To independently test this result, we exposed Math5>Cre; R26*flox*GFP embryos to a single pulse of EdU at E11, harvested their retinas at P1, and determined that 28% of strongly EdU+ cells in the GCL were GFP+ (Fig. 6D,E). As a third test, we evaluated retinas from early *Math5-lacZ*/+ embryos for coexpression of *lacZ* and Brn3b. The fraction of gal+ RGCs was relatively low at E11.5, consistent with the EB analysis, but increased from 20% to 60% between E11.5 and E13.5 (Fig. 7). Taken together, the results from these three experiments suggest that *Math5* is expressed by a subset of early neurogenic cells, and that only a fraction of Brn3b+ RGCs generated at E11-13 derive from the *Math5*+ cohort.

The *Math5*-independent early-born cells may express other proneural bHLH transcription factors in the Atonal family, such as Neurod1 or Neurog2. At E11.5, Neurod1 was detected in a pattern that partially overlaps *Math5-lacZ* (Suppl. Fig. 3), consistent with mRNA *in situ* hybridization data (Hufnagel et al., 2010). A similar overlap has been noted later in development (Kiyama et al., 2011; Le et al., 2006). This may explain the small number of

early-born Brn3b+ RGCs present in *Math5* −/− mice (Fig. 6B), as *Neurod1* can partially substitute for *Math5* function in RGC fate specification (Mao et al., 2008).

Symmetry of *Math5* expression in marked retroviral clones

During nervous system development, the mode of progenitor cell divisions changes over time (Gotz and Huttner, 2005; Huttner and Kosodo, 2005; Lu et al., 2000). Prior to neurogenesis, cell divisions predominantly follow the symmetric self-renewing mode (P-P), which expands the progenitor pool. During early neurogenesis, an asymmetric mode is frequently used to generate one mitotic daughter and one differentiating neuron (P-N). During late neurogenesis, most progenitors undergo a symmetric neurogenic mode of division (N-N), in which both daughters permanently exit the cell cycle. The fates adopted by neuronal daughters may also be symmetric (N_a-N_a) or asymmetric (N_a-N_b). In zebrafish, retinal progenitors expressing *ath5-GFP* undergo terminal neurogenic cell divisions (Poggi et al., 2005). These are symmetric with respect to *ath5-GFP* expression (N_{GFP}-N_{GFP}), but the daughters may have different cell fates, depending on the retinal environment.

To examine the mode of RPC division giving rise to *Math5+* daughter cells in mice, we infected retinal explants from E12.5 or E13.5 *Math5-lacZ/+* embryos with MSCV-IRES-GFP (MIG) retrovirus at low density to mark independent GFP+ clones. After culturing explants for 3 days *in vitro* (DIV), we immunostained 30 μm cryosections for GFP and βgal (*Math5-lacZ*), and determined the size and composition of clones containing at least one βgal+ cell ($N_{βgal}$) (Fig. 8A). These GFP+ clones ranged from 1 to 16 cells. We then focused our analysis on small clones (2-4 cell) containing ≥1 βgal+ cell, as these were most informative for symmetry of βgal+ expression. These clones are likely to represent terminal lineages, given their small size and time in culture. Indeed, all cells in these small clones were postmitotic, as judged by expression of the cell cycle inhibitor p27Kip1 (Dyer and Cepko, 2001) (data not shown). Among 23 clones scored, we observed both symmetric ($N_{βgal}$-$N_{βgal}$) (Fig. 8B,C) and asymmetric (N-$N_{βgal}$, or possibly P-$N_{βgal}$) (Fig. 8D) patterns of *Math5* expression. Of 23 informative neurogenic divisions, 13 (57%) were symmetric with respect to *Math5* expression and 10 were asymmetric (Fig. 8E). The fraction of symmetric divisions did not differ significantly between the E12.5 and E13.5 explant time-points (0.64 vs. 0.50 respectively, Fisher's exact test $P = 0.7$). Although few symmetric terminal divisions are expected at this age in the retina as a whole, the high frequency observed among the Math5+ cohort ($N_{βgal}$-$N_{βgal}$) in this small sample confirms that early progenitors are capable of N-N divisions in mice as in zebrafish (Poggi et al., 2005). Unlike zebrafish, neurogenic divisions can be asymmetric with respect to *Math5* expression in mice. These findings confirm that many retinal progenitors express *Math5* after terminal M phase.

DISCUSSION

Math5>Cre transgene recapitulates endogenous *Math5* expression

We believe that the Math5>Cre transgene is expressed in the same pattern as endogenous *Math5* mRNA for several reasons. First, the BAC transgenes that we examined are intact and contain >100 kb flanking *Math5* genomic DNA on both sides of the Cre cassette, while core regulatory elements for *Math5* retinal expression are located within 25 kb of the transcriptional start site (Ghiasvand et al., 2011; Hutcheson et al., 2005). Second, the spatiotemporal pattern of Z/AP activation is congruent with *Math5* mRNA and *Math5-lacZ* expression during retinal development. Third, all lineage-marked adult cells are born during the normal period of *Math5* expression, including rare 'late' cell types. Fourth, similar results were observed with independent BAC transgenic lines, suggesting that chromosomal position effects are minimal or nonexistent. Apart from the retina and RGC projections,

hPLAP staining was only noted in the cerebellum and in bushy cells of the cochlear nucleus, tissues that are known to express *Math5* mRNA (Saul et al., 2008). Fifth, the dual reporter concordance experiment provides no evidence for leaky or ectopic Cre expression. Sixth, a similar overall retinal pattern has been observed using a targeted Cre insertion (knock-in allele) in the *Math5* locus (Feng et al., 2010; Yang et al., 2003).

Our quantitative analysis significantly extends these previous studies and allows us to reach different conclusions regarding: [1] the size of the *Math5*-independent cohort of RGCs, [2] the relationship between *Math5* expression and cell cycle exit, [3] the role of *Math5* in determining non-RGC fates, and [4] the diversity of cell types within the Math5 lineage.

Math5>Cre does not mark all RGCs

Since *Math5* is necessary for RGC development, and functions as an intracellular factor, we expected all ganglion cells to be labeled by Cre, as descendants of *Math5+* progenitors. However, after carefully excluding displaced amacrine cells, we found that only 55% of RGCs were marked by the Math5>Cre transgene. A similar fraction of RGCs is likely to be labeled by the *Math5-Cre* knock-in allele (Feng et al., 2010) (*cf.* Suppl. Fig. 5D), although this finding was not originally appreciated (Yang et al., 2003). These *Math5* descendants project to all known target sites for RGCs in the brain (Fig. 2E), suggesting that they represent the ganglion cell population as a whole. There are two possible explanations for the incomplete marking of RGCs: [1] inefficiency of the *Cre-lox* system, and [2] the existence of a sizeable *Math5*-independent population of RGCs.

In principle, inefficient reporting may account for a substantial fraction of unlabeled RGCs in the birthdating and lineage tracing experiments. RGCs descending from *Math5+* precursors may escape detection for two reasons. First, the absolute level or duration of Cre expression in individual cells may not be sufficient to catalyze robust recombination. The Cre polypeptide must assemble into tetramers for enzymatic activity and has a short half-life in mammalian cells (Nagy, 2000). Generally speaking, Cre transgenes that are continuously active in differentiated cells are expected to be more efficient than those that are made briefly in a progenitor population. *Math5* is transiently expressed during retinal development (Fig. 1A) and may be transcribed for only a few hours in individual cells (Fig. 2F) (Fu et al., 2009). Consequently, in the dual concordance experiment, Math5>Cre activated only one reporter in 20% of marked cells (Fig. 4). However, because concordance was relatively high among all cell types (Suppl. Table 3), this effect cannot fully explain the incomplete labeling of RGCs. Second, some cells may epigenetically silence the Math5>Cre transgene or the *Math5-lacZ* allele, or may be otherwise globally resistant to Cre recombination. Indeed, we have observed rare mice with reduced or elevated RGC labeling (data not shown). In these retinas, the extent of labeling varied coordinately across different cell types, consistent with a clonal epigenetic effect. A similar variation has been noted among Tie1>Cre transgenic mice in the efficiency of endothelial cell labeling (Enge et al., 2002). Nonetheless, among the vast majority of Math5>Cre retinas, there was relatively little variation in the RGC labeling fraction (Table 1). Taken together, Cre inefficiency and epigenetic silencing are unlikely to explain the incomplete labeling of RGCs that we observed.

Alternatively, a subset of RGCs may develop independently of *Math5*. Detailed analysis of *Math5* −/− retinas has revealed a small population of widely dispersed ganglion cells, approximately 4% of wild-type, that survive to adulthood (Lin et al., 2004) and may project to the superior colliculi and laterial geniculate nuclei (Triplett et al., 2011). Moreover, recent data show that a related bHLH factor, Neurod1, can partially substitute for Math5 and allow RGC development (Mao et al., 2008). Indeed, we observed that fewer early-born cells express *Math5-lacZ* than Brn3b (Fig. 6B,C) and that many Brn3b+ RGCs at E11-E13 do not express *Math5-lacZ* (Fig. 7). A subset of nascent ganglion cells may develop from

Neurod1+ precursors (Suppl. Fig. 3), without *Math5.* Consistent with this idea, mutant mice lacking both factors mice have even fewer RGCs than *Math5* −/− mice (Kiyama et al., 2011).

The fraction of unmarked RGCs (~45%, Table 1) is 10-fold greater than the number of RGCs that survive in *Math5* −/− mice (~4%)(Lin et al., 2004). Apart from Cre inefficiency (noted above), there are two possible explanations for this discrepancy. First, RGCs derived from *Math5*+ progenitors may have a survival advantage during neonatal period (P0-P10) of ganglion cell apoptosis (Young, 1984). However, the deficiency of *Math5*-independent RGCs in *Math5* mutants was clearly evident early in retinal histogenesis, at E12.5 (Fig. 6B,C), well before the neonatal period of RGC culling. In addition, the fraction of *Math5*+ RGCs in P1 and adult retinas was the same, making this mechanism unlikely. Second, *Math5* lineage cells may have a substantial non-autonomous role in RGC fate specification or early differentiation. These cells may represent 'pioneering' neurons (Pittman et al., 2008; Raper and Mason, 2010), which promote axon pathfinding and fasciculation within the retina (Erskine and Herrera, 2007; Oster et al., 2004) and survival of *Math5*-independent RGCs. In the absence of *Math5*, cells in the inner retina undergo apoptosis during midgestation and surviving RGCs have severe pathfinding defects (Feng et al., 2010; Kiyama et al., 2011; Moshiri et al., 2008; Prasov and Glaser, 2009). Most likely, *Math5+* progenitors may favor the formation or survival of other RGCs by para- or juxtacrine signaling. Further work is needed to clarify molecular differences between the *Math5*+ cohort and other cells in the early retina.

Math5 is made by progenitors exiting the cell cycle

We have determined the precise relationship between onset of *Math5* expression and the cell cycle status of retinal progenitors (Fig. 9A). At early stages (<E14), *Math5-lacZ* was detected in some G2/M phase progenitors but was otherwise present only in non-proliferating cells. Based on the length of G2 phase (~ 2 hrs) (Sinitsina, 1971) and our analysis of retinal cell cycle kinetics in E13.5 Math5>Cre; R26*flox*GFP embryos, following a 30 min EdU pulse (Fig. 2G), we conclude that at least 15% (and up to 60%) of newly Math5+ cells (Cre+ GFP−) initiate expression before terminal M phase. During later stages (>E15), *Math5* was exclusively expressed in post-mitotic cells. *Math5* lineage cells did not re-enter the cell cycle at any stage, regardless of the *Math5* genotype. This comprehensive analysis reconciles previous disparate observations regarding the timing of *Math5* expression (Brown et al., 1998; Le et al., 2006; Yang et al., 2003), including RNA profiling of single retinal cells (Trimarchi et al., 2008). In recent studies, an HA epitope-tagged *Math5* allele was expressed with similar kinetics in early E12.5-E14.5 embryos, but was detected in more S, G2, and M phase cells than our *Math5-lacZ* allele (Feng et al., 2010; Kiyama et al., 2011; Wu et al., 2011). This is comparable to zebrafish, where *ath5-GFP* expression initiates during terminal S/G2 (Poggi et al., 2005), and is consistent with results obtained in frog and chick (Kay et al., 2001; Matter-Sadzinski et al., 2001; Perron et al., 1998; Poggi et al., 2005).

The variable timing of *Math5* expression was supported by clonal analysis. We observed symmetric *Math5-lacZ* expression in 13 of 23 informative divisions (56%, N_{Math5}-N_{Math5}) and asymmetric expression in the remaining clones (P/N-N_{Math5}). This frequency is convergent with cell cycle kinetic data discussed above. Together, these findings suggest that early progenitors giving rise to *Math5*+ cells are heterogeneous in their intrinsic properties and/or responses to the retinal microenvironment. By comparison, zebrafish *ath5* is expressed symmetrically in terminal neurogenic divisions (P_{ath5} N_{ath5}-N_{ath5}), but resulting daughters often adopt different fates (Poggi et al., 2005). This difference may be correlated with the accelerated pace of retinal neurogenesis in zebrafish compared to mice. Further

studies are needed to determine how the timing of *Math5* expression influences the fate choice of daughter cells in mice.

Math5 is unlikely to autonomously regulate the decision to exit the cell cycle for two reasons. First, it is variably expressed during or after the terminal division (Figs. 1B-D, 2G,H). Second, *Math5* lineage cells exhibit similar *lacZ* expression kinetics in mutant and wild-type mice (Fig. 1E-H). Instead, this binary choice must be made upstream or in parallel with *Math5* transcription. However, *Math5* may affect progenitor cycling indirectly. For example, differentiating RGCs secrete sonic hedgehog (Shh), which acts as a mitogen for RPCs and promotes rod and Müller glial fates (Jensen and Wallace, 1997; Levine et al., 1997; Wang et al., 2005; Yu et al., 2006). Accordingly, *Math5* mutants have thinner retinas with fewer rods and glia compared to wild-type mice (Brown et al., 2001), which may reflect a general loss of late-born cells. In zebrafish, *ath5* and *syu* (Shh) mutants exhibit similar defects in retinal cell mitosis, involving a delay in switching polarity of division, from central-peripheral (proliferative) to circumferential (neurogenic) modes (Das et al., 2003). This likewise suggests that nascent RGCs, not the *ath5* product *per se*, affect progenitor cell cycle dynamics.

Math5 establishes an RGC competence state

The expression fate mapping (Fig. 3) and dual concordance (Fig. 4) experiments support six conclusions. First, only a small fraction (3%) of the retina derives from *Math5*+ progenitors. Second, *Math5+* progenitors are multipotent. They retain the potential to generate all seven major retinal cell types. Third, *Math5+* progenitors contribute differentially to each cell type. The labeling frequency for a given cell type depends on the histogenic birth order and the temporal expression profile for *Math5* (Fig. 9B). Similar overall results were observed in a previous *Math5* lineage study (Feng et al., 2010; Yang et al., 2003). However, bipolars and Müller glia were not identified in the wild-type *Math5* lineage, presumably because fewer cells were sampled. Fourth, *Math5*+ progenitors express uniform levels of *Math5* and may represent a developmental equivalence group, similar to *ato*+ progenitors in the fly eye imaginal disc (Dokucu et al., 1996). Fifth, the fates of the *Math5*+ and *Math5*-populations change over time with parallel trajectories. The *Math5* lineage cells are biased in their selection of non-RGC fates, compared to other neurogenic cells in the same environment, but this difference does not depend on *Math5* activity. Sixth, the diversity of retinal cell fates within the *Math5* lineage was similar in mutant and wild-type mice, apart from the deficiency of RGCs (Fig. 9C). However, there were modest increases in the labeling fraction of rods, bipolar cells and Müller glia (Fig. 3I). The most parsimonious explanation for these quantitative effects is a difference between wild-type and mutant mice in the fractional distribution of cell types, creating a *denominator problem*. As noted above, *Math5* −/− retinas have significantly fewer late-born cells, presumably due to loss of Shh. Because all *Math5* lineage cells retain early birthdates in these retinas (Fig. 6C, Suppl. Fig. 2), this cohort appears expanded and skewed toward late cell fates. Taken together, we conclude *Math5* does not directly control the acquisition of multiple retinal cell fates (Feng et al., 2010). Instead, *Math5* has an active role in RGC fate specification, as a competence (permissive) factor, and a passive or minor role in the selection of alternative (non-RGC) fates.

Mechanisms of fate determination in the mouse retina

Retinal cell fate choice, differentiation and survival are jointly controlled by intrinsic and extrinsic factors (Livesey and Cepko, 2001). As a nuclear bHLH protein, Math5 is an intrinsic factor. It is necessary but not sufficient for RGC development. During retinogenesis, nine-fold more *Math5*+ cells are produced than develop into RGCs (Fig. 3, Table 1). These cells have a different fate bias than other neurogenic cells in the same

environment (Fig. 5). This property is conferred upstream of *Math5*. The development of RGCs from Math5+ cells may require the presence of positive cofactors or the absence of inhibitors. Soluble factors and cell-cell signaling are known to negatively regulate RGC genesis, including factors secreted by nascent RGCs (Austin et al., 1995; Belliveau and Cepko, 1999; Waid and McLoon, 1998; Zhang and Yang, 2001), and these may act on *Math5*+ cells. Together, our data suggest that the *Math5*+ cohort is influenced by intrinsic and extrinsic factors.

Our finding that *Math5*+ progenitors born on the same day can give rise to early or late cell types (Fig. 5) is consistent with a progressive restriction model for retinal neurogenesis, in which the progenitor pool is initially multipotent, but gradually loses competence to form early cell types (Pearson and Doe, 2003; Shen et al., 2006). This model is favored by heterochronic co-culture experiments (Reh, 1992; Watanabe and Raff, 1990) and *Ascl1* (*Mash1*) lineage analysis. Mouse *Ascl1*+ progenitors form all retinal cell types except RGCs (Brzezinski et al., 2011) and may represent the first competence-restricted state. However, our results are also consistent with a temporal restriction model, in which progenitors proceed *unidirectionally* in time through a relatively fixed series of competence states (Wong and Rapaport, 2009).

The reservoir of neurogenic cells that are competent to form RGCs greatly exceeds the final number. Likewise, the period of RGC competence extends beyond the normal time envelope for RGC births in rat and chick (James et al., 2003; Silva et al., 2003). This excess capacity, which includes *Math5*+ and *Math5*-cells, and the fate plasticity of *Math5*+ cells may serve to enhance the robustness of RGC development and ensure an appropriate histotypic profile in the mammalian retina.

Supplementary Material

Refer to Web version on PubMed Central for supplementary material.

Acknowledgments

The authors are grateful to Thom Saunders, Maggie van Keuren and the UM transgenic animal model core for generating the BAC transgenic animals; to Sue Tarlé and Dellaney Rudolph for technical support; to Nadean Brown for *in situ* hybridization data; to Nathaniel Heintz for BAC targeting plasmids and strains; to Sally Camper for the nlsCre plasmid; and to Sean Morrison for the MIG retroviral construct. The authors thank Chris Edwards, the UM microscopy and image analysis laboratory staff, Rafal Farjo and Mohammad Farah for technical advice. The authors are grateful to Nadean Brown, Chris Chou, David Turner, Matt Wilken, Julia Pollak, Anna La Torre, and Yumi Ueki for valuable discussions and critical reading of the manuscript. This research was funded by National Institutes of Health (NIH) R01 grant EY14259 (TG). JAB and LP were supported by NIH T32 grants EY13934 (JAB, LP), GM07544 (JAB), and GM07863 (LP).

REFERENCES

Adler R, Hatlee M. Plasticity and differentiation of embryonic retinal cells after terminal mitosis. Science. 1989; 243:391–3. [PubMed: 2911751]

Alexiades MR, Cepko C. Quantitative analysis of proliferation and cell cycle length during development of the rat retina. Dev Dyn. 1996; 205:293–307. [PubMed: 8850565]

Altshuler, DM.; Turner, DL.; Cepko, CL. Specification of cell type in the vertebrate retina. In: Lam, DMK.; Shatz, CJ., editors. Cell Lineage and Cell Fate in Visual System Development. MIT Press; Cambridge, MA: 1991. p. 37-58.

Austin CP, Feldman DE, Ida JA Jr. Cepko CL. Vertebrate retinal ganglion cells are selected from competent progenitors by the action of Notch. Development. 1995; 121:3637–50. [PubMed: 8582277]

Barnstable CJ, Hofstein R, Akagawa K. A marker of early amacrine cell development in rat retina. Brain Res. 1985; 352:286–90. [PubMed: 3896407]

Baye LM, Link BA. Nuclear migration during retinal development. Brain Res. 2008; 1192:29–36. [PubMed: 17560964]

Belliveau MJ, Cepko CL. Extrinsic and intrinsic factors control the genesis of amacrine and cone cells in the rat retina. Development. 1999; 126:555–66. [PubMed: 9876184]

Blanks JC, Johnson LV. Selective lectin binding of the developing mouse retina. J Comp Neurol. 1983; 221:31–41. [PubMed: 6643744]

Bradbury EM. Reversible histone modifications and the chromosome cell cycle. Bioessays. 1992; 14:9–16. [PubMed: 1312335]

Brown NL, Kanekar S, Vetter ML, Tucker PK, Gemza DL, Glaser T. Math5 encodes a murine basic helix-loop-helix transcription factor expressed during early stages of retinal neurogenesis. Development. 1998; 125:4821–33. [PubMed: 9806930]

Brown NL, Patel S, Brzezinski J, Glaser T. Math5 is required for retinal ganglion cell and optic nerve formation. Development. 2001; 128:2497–508. [PubMed: 11493566]

Brzezinski JAI, Brown NL, Tanikawa A, Bush RA, Sieving PA, Vitaterna M, Takahashi J, Glaser T. Abnormal circadian behavior and retinal electrophysiology in *Math5* mutant mice. Invest Ophthal Vis Sci. 2005; 46:2540–51. [PubMed: 15980246]

Brzezinski JA, Schulz SM, Crawford S, Wroblewski E, Brown NL, Glaser T. Math5 null mice have abnormal retinal and persistent hyaloid vasculatures. Dev Biol. 2003; 259:394.

Brzezinski JA, Kim EJ, Johnson JE, Reh TA. Ascl1 expression defines a subpopulation of lineage-restricted progenitors in the mammalian retina. Development. 2011; 138:3519–31. [PubMed: 21771810]

Buck SB, Bradford J, Gee KR, Agnew BJ, Clarke ST, Salic A. Detection of S-phase cell cycle progression using 5-ethynyl-2′-deoxyuridine incorporation with click chemistry, an alternative to using 5-bromo-2′-deoxyuridine antibodies. Biotechniques. 2008; 44:927–9. [PubMed: 18533904]

Carter-Dawson LD, LaVail MM. Rods and cones in the mouse retina. II. Autoradiographic analysis of cell generation using tritiated thymidine. J Comp Neurol. 1979; 188:263–72. [PubMed: 500859]

Cayouette M, Barres BA, Raff M. Importance of intrinsic mechanisms in cell fate decisions in the developing rat retina. Neuron. 2003; 40:897–904. [PubMed: 14659089]

Chen P, Johnson JE, Zoghbi HY, Segil N. The role of Math1 in inner ear development: Uncoupling the establishment of the sensory primordium from hair cell fate determination. Development. 2002; 129:2495–505. [PubMed: 11973280]

Cohen J. A coefficient of agreement for nominal scales. Educ Psychol Meas. 1960; 20:37–46.

Cushman LJ, Burrows HL, Seasholtz AF, Lewandoski M, Muzyczka N, Camper SA. Cre-mediated recombination in the pituitary gland. Genesis. 2000; 28:167–74. [PubMed: 11105060]

Das T, Payer B, Cayouette M, Harris WA. In vivo time-lapse imaging of cell divisions during neurogenesis in the developing zebrafish retina. Neuron. 2003; 37:597–609. [PubMed: 12597858]

Dokucu ME, Zipursky SL, Cagan RL. Atonal, rough and the resolution of proneural clusters in the developing Drosophila retina. Development. 1996; 122:4139–47. [PubMed: 9012533]

Drager UC. Birth dates of retinal ganglion cells giving rise to the crossed and uncrossed optic projections in the mouse. Proc R Soc Lond B Biol Sci. 1985; 224:57–77. [PubMed: 2581263]

Dyer MA, Cepko CL. p27Kip1 and p57Kip2 regulate proliferation in distinct retinal progenitor cell populations. J Neurosci. 2001; 21:4259–71. [PubMed: 11404411]

Dymecki, SM.; Rodriguez, CI.; Awatramani, RB. Switching on lineage tracers using site-specific recombination. In: Turksen, K., editor. Embryonic Stem Cells: Methods and Protocols. Vol. 185. Humana Press; 2002. p. 309-34.

Echelard Y, Vassileva G, McMahon AP. Cis-acting regulatory sequences governing Wnt-1 expression in the developing mouse CNS. Development. 1994; 120:2213–24. [PubMed: 7925022]

Enge M, Bjarnegard M, Gerhardt H, Gustafsson E, Kalen M, Asker N, Hammes HP, Shani M, Fassler R, Betsholtz C. Endothelium-specific platelet-derived growth factor-B ablation mimics diabetic retinopathy. Embo J. 2002; 21:4307–16. [PubMed: 12169633]

Erkman L, McEvilly RJ, Luo L, Ryan AK, Hooshmand F, O'Connell SM, Keithley EM, Rapaport DH, Ryan AF, Rosenfeld MG. Role of transcription factors Brn-3.1 and Brn-3.2 in auditory and visual system development. Nature. 1996; 381:603–6. [PubMed: 8637595]

Erskine L, Herrera E. The retinal ganglion cell axon's journey: insights into molecular mechanisms of axon guidance. Dev Biol. 2007; 308:1–14. [PubMed: 17560562]

Ezzeddine ZD, Yang X, DeChiara T, Yancopoulos G, Cepko CL. Postmitotic cells fated to become rod photoreceptors can be respecified by CNTF treatment of the retina. Development. 1997; 124:1055–67. [PubMed: 9056780]

Farah MH, Easter SS Jr. Cell birth and death in the mouse retinal ganglion cell layer. J Comp Neurol. 2005; 489:120–34. [PubMed: 15977166]

Feng L, Xie ZH, Ding Q, Xie X, Libby RT, Gan L. MATH5 controls the acquisition of multiple retinal cell fates. Mol Brain. 2010; 3:36. [PubMed: 21087508]

Fisher, RA. Statistical Methods for Research Workers. Oliver & Boyd; 1925.

Frankfort BJ, Mardon G. R8 development in the Drosophila eye: a paradigm for neural selection and differentiation. Development. 2002; 129:1295–306. [PubMed: 11880339]

Fu X, Kiyama T, Li R, Russell M, Klein WH, Mu X. Epitope-tagging Math5 and Pou4f2: new tools to study retinal ganglion cell development in the mouse. Dev Dyn. 2009; 238:2309–17. [PubMed: 19459208]

Fuhrmann S, Kirsch M, Hofmann HD. Ciliary neurotrophic factor promotes chick photoreceptor development in vitro. Development. 1995; 121:2695–706. [PubMed: 7671829]

Galli-Resta L, Ensini M. An intrinsic time limit between genesis and death of individual neurons in the developing retinal ganglion cell layer. J Neurosci. 1996; 16:2318–24. [PubMed: 8601811]

Gan L, Xiang M, Zhou L, Wagner DS, Klein WH, Nathans J. POU domain factor Brn-3b is required for the development of a large set of retinal ganglion cells. Proc Natl Acad Sci U S A. 1996; 93:3920–5. [PubMed: 8632990]

Gerfen, CR.; Holmes, A.; Sibley, D.; Skolnick, P.; Wray, S. Current Protocols in Neuroscience. John Wiley & Sons, Inc.; 2001. Common Stock Solutions, Buffers, and Media.

Ghiasvand NM, Rudolph DD, Mashayekhi M, Brzezinski J. A. t. Goldman D, Glaser T. Deletion of a remote enhancer near ATOH7 disrupts retinal neurogenesis, causing NCRNA disease. Nat Neurosci. 2011; 14:578–86. [PubMed: 21441919]

Goldowitz D, Rice DS, Williams RW. Clonal architecture of the mouse retina. Prog Brain Res. 1996; 108:3–15. [PubMed: 8979790]

Gomes FL, Zhang G, Carbonell F, Correa JA, Harris WA, Simons BD, Cayouette M. Reconstruction of rat retinal progenitor cell lineages in vitro reveals a surprising degree of stochasticity in cell fate decisions. Development. 2011; 138:227–35. [PubMed: 21148186]

Gong S, Yang XW, Li C, Heintz N. Highly efficient modification of bacterial artificial chromosomes (BACs) using novel shuttle vectors containing the R6Kgamma origin of replication. Genome Res. 2002; 12:1992–8. [PubMed: 12466304]

Gotz M, Huttner WB. The cell biology of neurogenesis. Nat Rev Mol Cell Biol. 2005; 6:777–88. [PubMed: 16314867]

Hatakeyama J, Kageyama R. Retrovirus-mediated gene transfer to retinal explants. Methods. 2002; 28:387–95. [PubMed: 12507456]

Hayden SA, Mills JW, Masland RM. Acetylcholine synthesis by displaced amacrine cells. Science. 1980; 210:435–7. [PubMed: 7433984]

Heintz N. BAC to the future: the use of bac transgenic mice for neuroscience research. Nat Rev Neurosci. 2001; 2:861–70. [PubMed: 11733793]

Helms AW, Abney AL, Ben-Arie N, Zoghbi HY, Johnson JE. Autoregulation and multiple enhancers control Math1 expression in the developing nervous system. Development. 2000; 127:1185–96. [PubMed: 10683172]

Holt CE, Bertsch TW, Ellis HM, Harris WA. Cellular determination in the Xenopus retina is independent of lineage and birth date. Neuron. 1988; 1:15–26. [PubMed: 3272153]

Hsiung F, Moses K. Retinal development in Drosophila: specifying the first neuron. Hum Mol Genet. 2002; 11:1207–14. [PubMed: 12015280]

Hu M, Krause D, Greaves M, Sharkis S, Dexter M, Heyworth C, Enver T. Multilineage gene expression precedes commitment in the hemopoietic system. Genes Dev. 1997; 11:774–85. [PubMed: 9087431]

Hufnagel RB, Le TT, Riesenberg AL, Brown NL. Neurog2 controls the leading edge of neurogenesis in the mammalian retina. Dev Biol. 2010; 340:490–503. [PubMed: 20144606]

Hutcheson DA, Hanson MI, Moore KB, Le TT, Brown NL, Vetter ML. bHLH-dependent and -independent modes of Ath5 gene regulation during retinal development. Development. 2005 in press.

Hutcheson DA, Vetter ML. The bHLH factors Xath5 and XNeuroD can upregulate the expression of XBrn3d, a POU-homeodomain transcription factor. Dev Biol. 2001; 232:327–38. [PubMed: 11401395]

Huttner WB, Kosodo Y. Symmetric versus asymmetric cell division during neurogenesis in the developing vertebrate central nervous system. Curr Opin Cell Biol. 2005; 17:648–57. [PubMed: 16243506]

James J, Das AV, Bhattacharya S, Chacko DM, Zhao X, Ahmad I. In vitro generation of early-born neurons from late retinal progenitors. J Neurosci. 2003; 23:8193–203. [PubMed: 12967980]

Jarman AP. Developmental genetics: vertebrates and insects see eye to eye. Curr Biol. 2000; 10:R857–9. [PubMed: 11114531]

Jensen AM, Wallace VA. Expression of Sonic hedgehog and its putative role as a precursor cell mitogen in the developing mouse retina. Development. 1997; 124:363–71. [PubMed: 9053312]

Jeon CJ, Strettoi E, Masland RH. The major cell populations of the mouse retina. J Neurosci. 1998; 18:8936–46. [PubMed: 9786999]

Kageyama R, Nakanishi S. Helix-loop-helix factors in growth and differentiation of the vertebrate nervous system. Curr Opin Genet Dev. 1997; 7:659–65. [PubMed: 9388783]

Kanekar S, Perron M, Dorsky R, Harris WA, Jan LY, Jan YN, Vetter ML. Xath5 participates in a network of bHLH genes in the developing Xenopus retina. Neuron. 1997; 19:981–94. [PubMed: 9390513]

Kay JN, Finger-Baier KC, Roeser T, Staub W, Baier H. Retinal ganglion cell genesis requires lakritz, a Zebrafish atonal Homolog. Neuron. 2001; 30:725–36. [PubMed: 11430806]

Key G, Becker MH, Baron B, Duchrow M, Schluter C, Flad HD, Gerdes J. New Ki-67-equivalent murine monoclonal antibodies (MIB 1-3) generated against bacterially expressed parts of the Ki-67 cDNA containing three 62 base pair repetitive elements encoding for the Ki-67 epitope. Lab Invest. 1993; 68:629–36. [PubMed: 7685843]

Khor CC, Ramdas WD, Vithana EN, Cornes BK, Sim X, Tay WT, Saw SM, Zheng Y, Lavanya R, Wu R, Wang JJ, Mitchell P, Uitterlinden AG, Rivadeneira F, Teo YY, Chia KS, Seielstad M, Hibberd M, Vingerling JR, Klaver CC, Jansonius NM, Tai ES, Wong TY, van Duijn CM, Aung T. Genome-wide association studies in Asians confirm the involvement of ATOH7 and TGFBR3, and further identify CARD10 as a novel locus influencing optic disc area. Hum Mol Genet. 2011; 20:1864–72. [PubMed: 21307088]

Kiyama T, Mao CA, Cho JH, Fu X, Pan P, Mu X, Klein WH. Overlapping spatiotemporal patterns of regulatory gene expression are required for neuronal progenitors to specify retinal ganglion cell fate. Vision Res. 2011; 51:251–9. [PubMed: 20951721]

LaVail MM, Faktorovich EG, Hepler JM, Pearson KL, Yasumura D, Matthes MT, Steinberg RH. Basic fibroblast growth factor protects photoreceptors from light-induced degeneration in albino rats. Ann N Y Acad Sci. 1991; 638:341–7. [PubMed: 1785811]

Le TT, Wroblewski E, Patel S, Riesenberg AN, Brown NL. Math5 is required for both early retinal neuron differentiation and cell cycle progression. Dev Biol. 2006; 295:764–78. [PubMed: 16690048]

Levine EM, Roelink H, Turner J, Reh TA. Sonic hedgehog promotes rod photoreceptor differentiation in mammalian retinal cells in vitro. J Neurosci. 1997; 17:6277–88. [PubMed: 9236238]

Lin B, Wang SW, Masland RH. Retinal ganglion cell type, size, and spacing can be specified independent of homotypic dendritic contacts. Neuron. 2004; 43:475–85. [PubMed: 15312647]

Liu W, Mo Z, Xiang M. The Ath5 proneural genes function upstream of Brn3 POU domain transcription factor genes to promote retinal ganglion cell development. Proc Natl Acad Sci U S A. 2001; 98:1649–54. [PubMed: 11172005]

Livak KJ, Schmittgen TD. Analysis of relative gene expression data using real-time quantitative PCR and the 2(-Delta Delta C(T)) Method. Methods. 2001; 25:402–8. [PubMed: 11846609]

Livesey FJ, Cepko CL. Vertebrate neural cell-fate determination: lessons from the retina. Nat Rev Neurosci. 2001; 2:109–18. [PubMed: 11252990]

Lobe CG, Koop KE, Kreppner W, Lomeli H, Gertsenstein M, Nagy A. Z/AP, a double reporter for cre-mediated recombination. Dev Biol. 1999; 208:281–92. [PubMed: 10191045]

Lu B, Jan L, Jan YN. Control of cell divisions in the nervous system: symmetry and asymmetry. Annu Rev Neurosci. 2000; 23:531–56. [PubMed: 10845074]

Macgregor S, Hewitt AW, Hysi PG, Ruddle JB, Medland SE, Henders AK, Gordon SD, Andrew T, McEvoy B, Sanfilippo PG, Carbonaro F, Tah V, Li YJ, Bennett SL, Craig JE, Montgomery GW, Tran-Viet KN, Brown NL, Spector TD, Martin NG, Young TL, Hammond CJ, Mackey DA. Genome-wide association identifies ATOH7 as a major gene determining human optic disc size. Hum Mol Genet. 2010; 19:2716–24. [PubMed: 20395239]

Mao CA, Wang SW, Pan P, Klein WH. Rewiring the retinal ganglion cell gene regulatory network: Neurod1 promotes retinal ganglion cell fate in the absence of Math5. Development. 2008; 135:3379–88. [PubMed: 18787067]

Mao X, Fujiwara Y, Chapdelaine A, Yang H, Orkin SH. Activation of EGFP expression by Cre-mediated excision in a new ROSA26 reporter mouse strain. Blood. 2001; 97:324–6. [PubMed: 11133778]

Masai I. [Mechanisms underlying induction and progression of a neurogenic wave in the zebrafish developing retina]. Tanpakushitsu Kakusan Koso. 2000; 45:2782–90. [PubMed: 11187780]

Matter-Sadzinski L, Matter JM, Ong MT, Hernandez J, Ballivet M. Specification of neurotransmitter receptor identity in developing retina: the chick ATH5 promoter integrates the positive and negative effects of several bHLH proteins. Development. 2001; 128:217–31. [PubMed: 11124117]

Mayer W, Smith A, Fundele R, Haaf T. Spatial separation of parental genomes in preimplantation mouse embryos. J Cell Biol. 2000; 148:629–34. [PubMed: 10684246]

McLoon SC, Barnes RB. Early differentiation of retinal ganglion cells: an axonal protein expressed by premigratory and migrating retinal ganglion cells. J Neurosci. 1989; 9:1424–32. [PubMed: 2703885]

Miller MW, Nowakowski RS. Use of bromodeoxyuridine-immunohistochemistry to examine the proliferation, migration and time of origin of cells in the central nervous system. Brain Res. 1988; 457:44–52. [PubMed: 3167568]

Moshiri A, Gonzalez E, Tagawa K, Maeda H, Wang M, Frishman LJ, Wang SW. Near complete loss of retinal ganglion cells in the math5/brn3b double knockout elicits severe reductions of other cell types during retinal development. Dev Biol. 2008; 316:214–27. [PubMed: 18321480]

Mu X, Beremand PD, Zhao S, Pershad R, Sun H, Scarpa A, Liang S, Thomas TL, Klein WH. Discrete gene sets depend on POU domain transcription factor Brn3b/Brn-3.2/POU4f2 for their expression in the mouse embryonic retina. Development. 2004; 131:1197–1210. [PubMed: 14973295]

Mu X, Fu X, Beremand PD, Thomas TL, Klein WH. Gene regulation logic in retinal ganglion cell development: Isl1 defines a critical branch distinct from but overlapping with Pou4f2. Proc Natl Acad Sci U S A. 2008; 105:6942–7. [PubMed: 18460603]

Nagy A. Cre recombinase: the universal reagent for genome tailoring. Genesis. 2000; 26:99–109. [PubMed: 10686599]

Oster SF, Deiner M, Birgbauer E, Sretavan DW. Ganglion cell axon pathfinding in the retina and optic nerve. Semin Cell Dev Biol. 2004; 15:125–36. [PubMed: 15036215]

Pan L, Deng M, Xie X, Gan L. ISL1 and BRN3B co-regulate the differentiation of murine retinal ganglion cells. Development. 2008; 135:1981–90. [PubMed: 18434421]

Pear W. Transient transfection methods for preparation of high-titer retroviral supernatants. Curr Protoc Mol Biol. 2001 Chapter 9, Unit9 11.

Pearson BJ, Doe CQ. Regulation of neuroblast competence in Drosophila. Nature. 2003; 425:624–8. [PubMed: 14534589]

Peichl L, Gonzalez-Soriano J. Unexpected presence of neurofilaments in axon-bearing horizontal cells of the mammalian retina. J Neurosci. 1993; 13:4091–100. [PubMed: 8366362]

Peichl L, Gonzalez-Soriano J. Morphological types of horizontal cell in rodent retinae: a comparison of rat, mouse, gerbil, and guinea pig. Vis Neurosci. 1994; 11:501–17. [PubMed: 8038125]

Perron M, Kanekar S, Vetter ML, Harris WA. The genetic sequence of retinal development in the ciliary margin of the Xenopus eye. Dev Biol. 1998; 199:185–200. [PubMed: 9698439]

Perry VH, Walker M. Amacrine cells, displaced amacrine cells and interplexiform cells in the retina of the rat. Proc R Soc Lond B Biol Sci. 1980; 208:415–31. [PubMed: 6158054]

Pittman AJ, Law MY, Chien CB. Pathfinding in a large vertebrate axon tract: isotypic interactions guide retinotectal axons at multiple choice points. Development. 2008; 135:2865–71. [PubMed: 18653554]

Poggi L, Vitorino M, Masai I, Harris WA. Influences on neural lineage and mode of division in the zebrafish retina in vivo. J Cell Biol. 2005; 171:991–9. [PubMed: 16365165]

Prasov L, Brown NL, Glaser T. A critical analysis of Atoh7 (Math5) mRNA splicing in the developing mouse retina. PLoS One. 2010; 5:e12315. [PubMed: 20808762]

Prasov L, Glaser T. Math5 Confers Multipotency to Fate-Restricted Post-Mitotic Retinal Precursors. ARVO Meeting Abstracts. 2009; 50:1310.

Rachel RA, Dolen G, Hayes NL, Lu A, Erskine L, Nowakowski RS, Mason CA. Spatiotemporal features of early neuronogenesis differ in wild-type and albino mouse retina. J Neurosci. 2002; 22:4249–63. [PubMed: 12040030]

Ramdas WD, van Koolwijk LM, Ikram MK, Jansonius NM, de Jong PT, Bergen AA, Isaacs A, Amin N, Aulchenko YS, Wolfs RC, Hofman A, Rivadeneira F, Oostra BA, Uitterlinden AG, Hysi P, Hammond CJ, Lemij HG, Vingerling JR, Klaver CC, van Duijn CM. A genome-wide association study of optic disc parameters. PLoS Genet. 2010; 6:e1000978. [PubMed: 20548946]

Rapaport DH, Patheal SL, Harris WA. Cellular competence plays a role in photoreceptor differentiation in the developing Xenopus retina. J Neurobiol. 2001; 49:129–41. [PubMed: 11598920]

Rapaport DH, Wong LL, Wood ED, Yasumura D, LaVail MM. Timing and topography of cell genesis in the rat retina. J Comp Neurol. 2004; 474:304–24. [PubMed: 15164429]

Raper J, Mason C. Cellular strategies of axonal pathfinding. Cold Spring Harb Perspect Biol. 2010; 2:a001933. [PubMed: 20591992]

Reese BE, Colello RJ. Neurogenesis in the retinal ganglion cell layer of the rat. Neuroscience. 1992; 46:419–29. [PubMed: 1542415]

Reh TA. Cellular interactions determine neuronal phenotypes in rodent retinal cultures. J Neurobiol. 1992; 23:1067–83. [PubMed: 1460465]

Reh TA, Kljavin IJ. Age of differentiation determines rat retinal germinal cell phenotype: induction of differentiation by dissociation. J Neurosci. 1989; 9:4179–89. [PubMed: 2592995]

Repka AM, Adler R. Accurate determination of the time of cell birth using a sequential labeling technique with [3H]-thymidine and bromodeoxyuridine (“window labeling”). J Histochem Cytochem. 1992; 40:947–53. [PubMed: 1607643]

Rodieck, RW. The First Steps in Seeing. Sinauer; Sunderland, MA: 1998.

Saul SM, Brzezinski J. A. t. Altschuler RA, Shore SE, Rudolph DD, Kabara LL, Halsey KE, Hufnagel RB, Zhou J, Dolan DF, Glaser T. Math5 expression and function in the central auditory system. Mol Cell Neurosci. 2008; 37:153–69. [PubMed: 17977745]

Schneider ML, Turner DL, Vetter ML. Notch signaling can inhibit Xath5 function in the neural plate and developing retina. Mol Cell Neurosci. 2001; 18:458–72. [PubMed: 11922138]

Shen Q, Wang Y, Dimos JT, Fasano CA, Phoenix TN, Lemischka IR, Ivanova NB, Stifani S, Morrisey EE, Temple S. The timing of cortical neurogenesis is encoded within lineages of individual progenitor cells. Nat Neurosci. 2006; 9:743–51. [PubMed: 16680166]

Sidman, RL. Histogenesis of mouse retina studied with thymidine-H3. In: Smelser, GK., editor. Structure of the Eye. Academic Press; New York: 1961. p. 487-506.

Silva AO, Ercole CE, McLoon SC. Regulation of ganglion cell production by Notch signaling during retinal development. J Neurobiol. 2003; 54:511–24. [PubMed: 12532401]

Simpson JI. The accessory optic system. Annu Rev Neurosci. 1984; 7:13–41. [PubMed: 6370078]

Sinitsina VF. [DNA synthesis and cell population kinetics in embryonal histogenesis of the retina in mice]. Arkh Anat Gistol Embriol. 1971; 61:58–67. [PubMed: 5158168]

Snow RL, Robson JA. Ganglion cell neurogenesis, migration and early differentiation in the chick retina. Neuroscience. 1994; 58:399–409. [PubMed: 8152546]

Sun Y, Kanekar SL, Vetter ML, Gorski S, Jan YN, Glaser T, Brown NL. Conserved and divergent functions of Drosophila atonal, amphibian, and mammalian Ath5 genes. Evol Dev. 2003; 5:532–41. [PubMed: 12950631]

Swift S, Lorens J, Achacoso P, Nolan GP. Rapid production of retroviruses for efficient gene delivery to mammalian cells using 293T cell-based systems. Curr Protoc Immunol. 2001 Chapter 10, Unit 10 17C.

Trimarchi JM, Stadler MB, Cepko CL. Individual retinal progenitor cells display extensive heterogeneity of gene expression. PLoS One. 2008; 3:e1588. [PubMed: 18270576]

Triplett JW, Pfeiffenberger C, Yamada J, Stafford BK, Sweeney NT, Litke AM, Sher A, Koulakov AA, Feldheim DA. Competition is a driving force in topographic mapping. Proc Natl Acad Sci U S A. 2011

Turner DL, Cepko CL. A common progenitor for neurons and glia persists in rat retina late in development. Nature. 1987; 328:131–6. [PubMed: 3600789]

Turner DL, Snyder EY, Cepko CL. Lineage-independent determination of cell type in the embryonic mouse retina. Neuron. 1990; 4:833–45. [PubMed: 2163263]

Van Parijs L, Refaeli Y, Lord JD, Nelson BH, Abbas AK, Baltimore D. Uncoupling IL-2 signals that regulate T cell proliferation, survival, and Fas-mediated activation-induced cell death. Immunity. 1999; 11:281–8. [PubMed: 10514006]

von Bohlen und Halbach O. The isolated mammalian brain: an in vivo preparation suitable for pathway tracing. Eur J Neurosci. 1999; 11:1096–100. [PubMed: 10103102]

Waid DK, McLoon SC. Ganglion cells influence the fate of dividing retinal cells in culture. Development. 1998; 125:1059–66. [PubMed: 9463352]

Wang SW, Kim BS, Ding K, Wang H, Sun D, Johnson RL, Klein WH, Gan L. Requirement for math5 in the development of retinal ganglion cells. Genes Dev. 2001; 15:24–9. [PubMed: 11156601]

Wang SW, Mu X, Bowers WJ, Klein WH. Retinal ganglion cell differentiation in cultured mouse retinal explants. Methods. 2002; 28:448–56. [PubMed: 12507463]

Wang Y, Dakubo GD, Thurig S, Mazerolle CJ, Wallace VA. Retinal ganglion cell-derived sonic hedgehog locally controls proliferation and the timing of RGC development in the embryonic mouse retina. Development. 2005; 132:5103–13. [PubMed: 16236765]

Wang Y, Smallwood PM, Cowan M, Blesh D, Lawler A, Nathans J. Mutually exclusive expression of human red and green visual pigment-reporter transgenes occurs at high frequency in murine cone photoreceptors. Proc Natl Acad Sci U S A. 1999; 96:5251–6. [PubMed: 10220452]

Watanabe M, Rutishauser U, Silver J. Formation of the retinal ganglion cell and optic fiber layers. J Neurobiol. 1991; 22:85–96. [PubMed: 2010752]

Watanabe T, Raff MC. Rod photoreceptor development in vitro: intrinsic properties of proliferating neuroepithelial cells change as development proceeds in the rat retina. Neuron. 1990; 4:461–7. [PubMed: 2138470]

Wee R, Castrucci AM, Provencio I, Gan L, Van Gelder RN. Loss of photic entrainment and altered free-running circadian rhythms in math5−/− mice. J Neurosci. 2002; 22:10427–33. [PubMed: 12451142]

Wessells, NK. Tissue Interactions and Development. W.A. Benjamin; Menlo Park, CA: 1977.

Wetts R, Fraser SE. Multipotent precursors can give rise to all major cell types of the frog retina. Science. 1988; 239:1142–5. [PubMed: 2449732]

Wong LL, Rapaport DH. Defining retinal progenitor cell competence in Xenopus laevis by clonal analysis. Development. 2009; 136:1707–15. [PubMed: 19395642]

Wu F, Sapkota D, Li R, Mu X. Onecut 1 and onecut 2 are potential regulators of mouse retinal development. J Comp Neurol. 2011

Yang K, Hitomi M, Stacey DW. Variations in cyclin D1 levels through the cell cycle determine the proliferative fate of a cell. Cell Div. 2006; 1:32. [PubMed: 17176475]

Yang XJ. Roles of cell-extrinsic growth factors in vertebrate eye pattern formation and retinogenesis. Semin Cell Dev Biol. 2004; 15:91–103. [PubMed: 15036212]

Yang Z, Ding K, Pan L, Deng M, Gan L. Math5 determines the competence state of retinal ganglion cell progenitors. Dev Biol. 2003; 264:240–54. [PubMed: 14623245]

Young RW. Cell death during differentiation of the retina in the mouse. J Comp Neurol. 1984; 229:362–73. [PubMed: 6501608]

Young RW. Cell differentiation in the retina of the mouse. Anat Rec. 1985; 212:199–205. [PubMed: 3842042]

Young TL, Cepko CL. A role for ligand-gated ion channels in rod photoreceptor development. Neuron. 2004; 41:867–79. [PubMed: 15046720]

Yu C, Mazerolle CJ, Thurig S, Wang Y, Pacal M, Bremner R, Wallace VA. Direct and indirect effects of hedgehog pathway activation in the mammalian retina. Mol Cell Neurosci. 2006; 32:274–82. [PubMed: 16815712]

Zhang XM, Yang XJ. Regulation of retinal ganglion cell production by Sonic hedgehog. Development. 2001; 128:943–57. [PubMed: 11222148]

Highlights

- Math5 bHLH factor confers ganglion cell competence on retinal progenitor cells
- Math5 is expressed in neurogenic cells during terminal G2 phase or early G0
- Quantitative Math5>Cre lineage analysis and birthdating in wildtype and mutant mice
- Identification of Math5-independent ganglion cells
- Math5 does not actively determine non-RGC fates

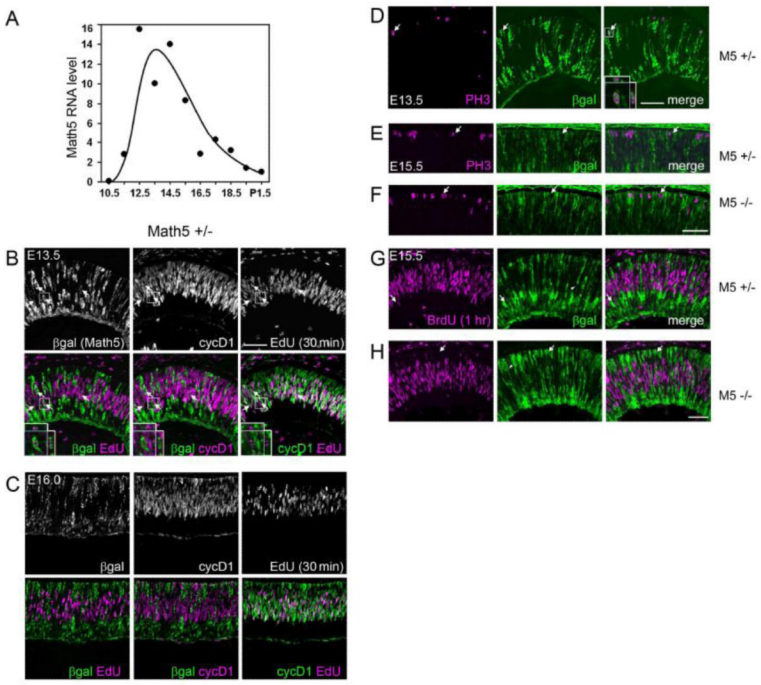

Fig. 1.

Math5 is expressed by early retinal progenitors during or shortly following their terminal cell cycle. (A) Time course of *Math5* mRNA expression in developing eyes. *Math5* mRNA levels peak at E14, with a profile that resembles RGC birthdating curves (Young 1985; Rapaport *et al.* 2004). (B-C) Sections from E13.5 (B) or E16.0 (C) *Math5* +/− embryos co-stained for βgal (*Math5-lacZ* allele), EdU (following a 30 min chase), and cyclin D1 (marks G1/early S phase). Upper and lower panels show single- and double-labeled confocal projection images of 10 (B) or 3 (C) 1-m optical slices. Insets show a βgal+ cell in G2 (EdU + cyclinD1−). At E13.5, some βgal+ EdU+ cells are present (arrows, 18 of 517 βgal+ cells), but none are cyclinD1+ (0 of 517). At E16.0, few or no βgal+ cells are EdU+ or cycD1+. (D-H) Retinal sections from *Math5* +/− (D, E, G) and *Math5* −/− (E, G) mice co-stained for βgal and cell cycle markers. *Math5-lacZ* is occasionally co-expressed with M-phase marker PH3 at E13.5 (arrow in D, inset), but does not overlap with PH3 (arrows in E,F) or BrdU (1 hr chase) (arrows in G,H) at E15.5. Therefore, *Math5-lacZ* expression initiates during terminal G2 phase at E13.5, but after terminal M phase at E15.5 and E16.0 in both *Math5* +/− and −/− retinas. M5, *Math5*; βgal, *E. coli* β-galactosidase; cycD1, cyclinD1; PH3, phosphohistone H3. Scale bar, 50 m.

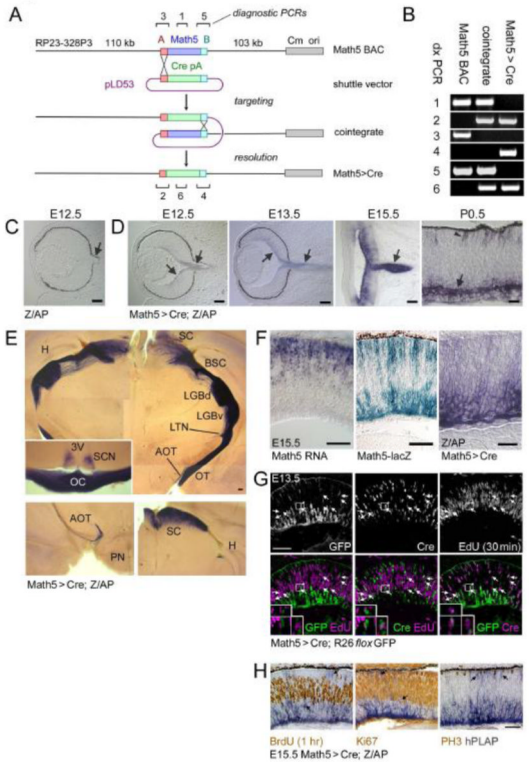

Fig. 2.

Construction and expression of the Math5>Cre transgene. (A) Math5>Cre BACs were generated in *E. coli* by a two-step homologous recombination procedure. The single-exon *Math5* open reading frame was precisely replaced with a nlsCre-pA cassette, using “A” and “B” homology arms derived from 5′ (red box) and 3′ (cyan box) UTRs. The pLD53 shuttle vector contains *recA* recombinase, positive (*amp*) and negative (*sacB*) selection cassettes, and the R6K origin of replication. The pBACe3.6 vector (gray box) contains the chloramphenicol resistance gene (*Cm*) and P1 origin (*ori*). (B) Confirmation of recombinant BAC structure using diagnostic (dx) PCRs 1-6 indicated in panel A (assembled from multiple gels). (C-F) Developmental expression pattern. Math5>Cre mice were crossed to mice carrying the Z/AP transgene, which permanently reports Cre activity. Alkaline phosphatase (hPLAP)-positive RGCs (purple, arrows) are first observed at E12.5 in double transgenic embryos (D), while control littermates (C) containing only the Z/AP transgene are negative. hPLAP activity increases from E13.5 to E15.5 as RGCs develop and form the optic nerve. By P0.5, hPLAP activity is abundant in RGCs (arrow) and can be detected in some photoreceptors (arrowhead); however most of the retina is unlabeled. (E) Composite images of 250 μm coronal vibratome sections through the adult thalamus and optic chiasm (inset) show the axonal projections of RGCs derived from *Math5+* precursors. Lower panels show sections through the accesory optic system (left) and superior colliculus (right). Labeled RGCs project to all major ganglion cell target sites in the CNS. No significant staining was observed in the cerebral cortex or hippocampus. (F) Kinetics of *Math5* expression in the E15.5 retina. *Math5* mRNA (*in situ* hybridization) is expressed in retinal progenitor cells, while the cytoplasmic *Math5-lacZ* knock-in allele labels progenitors (sclerad) and developing RGCs (vitread), which have recently transcribed *Math5* (β-galactosidase activity). hPLAP activity in Math5>Cre; Z/AP mice is localized to developing RGCs on the vitread side of the retinal epithelium. These patterns demonstrate the spatiotemporal progression of *Math5* expression, if one considers the perdurance of β-galactosidase, the delay associated with Cre excision, and interkinetic nuclear migration.

Math5 is expressed transiently in progenitors that become RGCs. (G-H) Math5>Cre retinas co-stained for lineage tracers and cell cycle markers. Cre is expressed with the same kinetics as *Math5*, whereas GFP or hPLAP reporters are expressed with a delay. (G) At E13.5, Cre+ EdU+ cells are present (30 min chase, arrows, 33 of 394 Cre+ cells), but no GFP+ EdU+ cells are observed (0 of 309 GFP+ cells). (H) At E15.5, no hPLAP+ cells (arrows) are co-labeled with BrdU (1 hr chase), PH3, or Ki67 (marks late G1 through M phase). Together, these results indicate that cells in the *Math5* lineage do not re-enter the cell cycle. pA, polyadenylation signal; SC, superior colliculus; BSC, brachium of the superior colliculus; LGB_d, lateral geniculate body, pars dorsalis; LGB_v, lateral geniculate body, pars ventralis; LTN, lateral terminal nucleus; AOT, accessory optic tract; OT, optic tract; TV, third ventricle; SCN, suprachiasmatic nucleus; OC, optic chiasm; H, hippocampus; PN, pons. Scale bars, 100 m in C-F; 50 m in G-H.

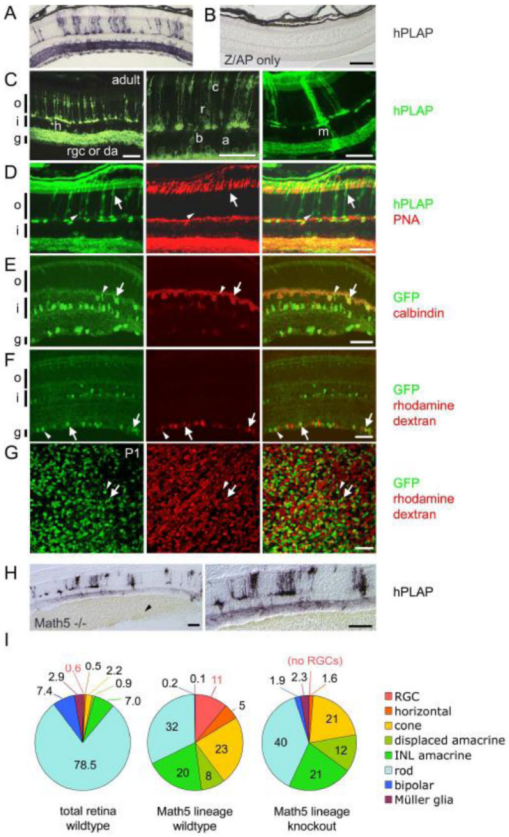

Fig. 3.

Math5+ progenitors contribute differentially to all retinal cell types. Math5>Cre mice were crossed to Z/AP (A-D) or R26*flox*GFP reporter (E-G) strains. (A) In Math5>Cre; Z/AP mice, hPLAP+ descendants of *Math5+* progenitors represent 3% of adult retinal cells (see Table 1) and are present in every cell layer. (B) Z/AP-only control retinas have no hPLAP activity. (C) *Math5+* descendants, detected by hPLAP immunostaining, include horizontal (h), ganglion (rgc), displaced amacrine (da), INL amacrine (a), bipolar (b), rod (r), cone (c) and Müller glial (m) cells. (D) *Math5+* cone (arrows) and rod (arrowheads) photoreceptors are distinguished by co-labeling with anti-hPLAP and cone-specific PNA lectin. Non-specific labeling of pigment epithelium and choroid reflects mouse IgG crossreactivity. (E-G) In Math5>Cre; R26*flox*GFP mice, Math5+ horizontal cells (E, arrows) are marked by GFP and calbindin immunoreactivity. The arrowhead shows a solitary *Math5+* bipolar cell. (F-G) *Math5+* RGCs (arrows) and displaced amacrines (arrowheads) in the GCL are shown in adult retinal sections (F) or P1 retinal flatmounts (G). RGCs are distinguished by retrograde labeling of optic nerve axons with rhodamine dextran. There is no difference in the GFP+ fraction of rhodamine dextran-labeled RGCs between these two ages. (H) The fate of Math5>Cre-expressing progenitors in *Math5* −/− mice. hPLAP+ cells are distributed throughout the retina, but RGCs are lacking. Vitreal hemorrhages (arrowhead) are common in *Math5*−/− mice. (I) The distribution of cell fates in the entire retina (from Jeon et al., 1998), in the *Math5* lineage of wild-type mice, and in the *Math5* lineage of knockout mice. The *Math5* lineage is biased toward early-born cell types (RGC, horizontal, cone), although rods are the most common fate adopted by *Math5+* cells. In the *Math5* knockout, lineage-derived cells adopt all retinal fates except for RGCs. hPLAP, human placental alkaline phosphatase; o, outer nuclear layer; i, inner nuclear layer; g, ganglion cell layer. Scale bars, 100 m in A-B, H; 50 m in C-G.

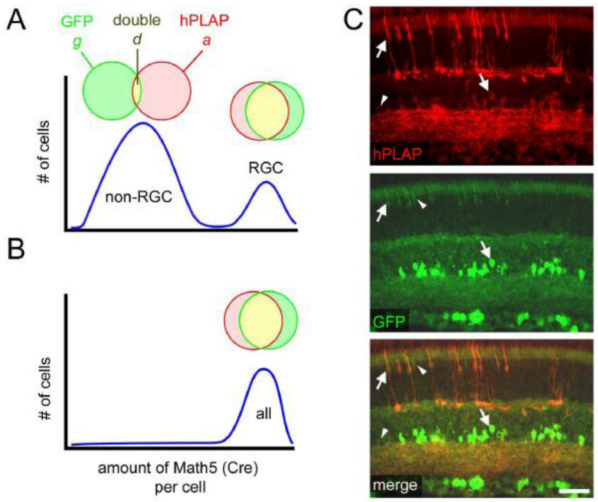

D

	labeled fraction		reporter concordance		
cells	single (ρ)	joint (ρ^2)	expected*	observed*	Cohen's κ
GCL	0.40	0.16	0.25	0.77	0.70
cone	0.31	0.095	0.18	0.84	0.80
INL Am	0.09	0.007	0.04	0.80	0.79
rod	0.012	0.0001	0.006	0.82	0.82

$$* \text{expected} = \frac{\rho^2}{(2\rho - \rho^2)} \qquad * \text{observed} = \frac{d}{a + g - d}$$

Fig. 4.

All Math5>Cre progenitors express similar levels of Cre, regardless of cell fate. Math5>Cre lineage analysis was performed using Z/AP and R26*flox*GFP reporters simultaneously, to evaluate the heterogeneity of *Math5* expression among progenitors. This analysis assumes that the probability of reporter activation in a given cell is determined by the cumulative amount of Cre recombinase expressed by that cell. (A-B) Two models for *Math5* (Cre) expression. (A) Bimodal expression. In this model, *Math5+* progenitors giving rise to non-ganglion cell types express Cre weakly (left peak), so reporter activation in these cells is inefficient, and consequently few of their descendants co-express GFP and hPLAP. RGCs in the same retinas express Cre strongly (right peak) and are expected to have high concordance. (B) Uniform expression. In this model, every *Math5+* progenitor expresses Cre strongly, so concordance is very high for all cell types (B, right). (C) Retinas of adult Math5>Cre; Z/AP; R26*flox*GFP mice immunostained for hPLAP and GFP. Double-labeled cells (arrows) greatly outnumber single-labeled cells (arrowheads). (D) The observed concordance between hPLAP and GFP reporters was ~80%, which is significantly greater than expected by chance (Cohen's $\kappa > 0.7$). This value was similar for all cell types, indicating that *Math5* is expressed at uniform levels by a subpopulation of progenitor cells, only some of which develop as RGCs. The labeled fractions (ρ) are based on data in Table 1. GCL includes RGCs and displaced amacrines; INL Am, inner nuclear layer amacrine. Scale bar, 50 m.

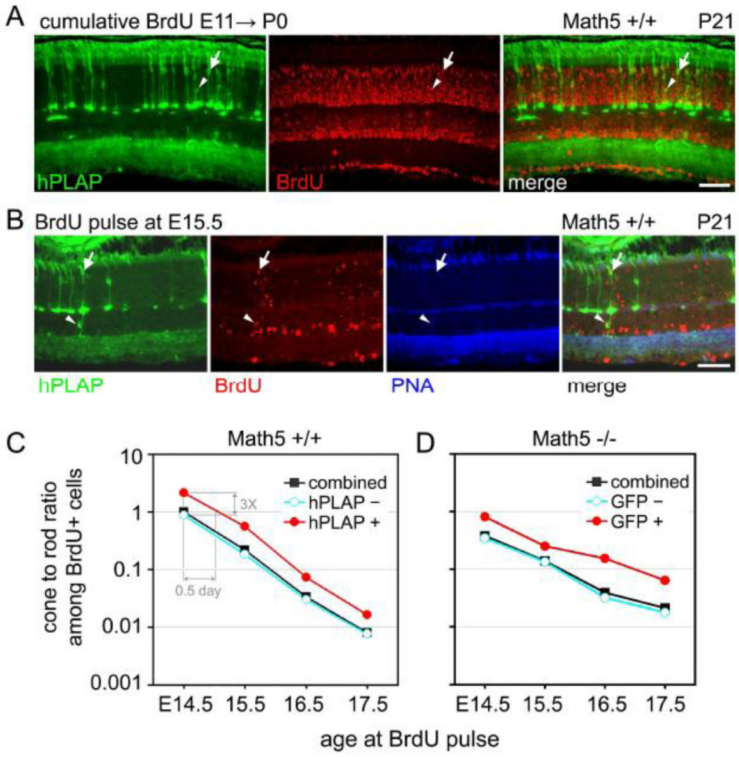

Fig. 5.

The fate distribution of *Math5+* progenitors changes over time. (A) Cumulative BrdU labeling experiment. Math5>Cre; Z/AP embryos were continuously exposed to BrdU from E10.5 to P0 and their retinas were collected at P21. Nearly all *Math5+* descendants (hPLAP +) are heavily labeled with BrdU, indicating that the majority exited mitosis before P0, including lineage-labeled cones (arrows) and rods (arrowheads). There is a distinct gradient of BrdU labeling (birthdates) within the inner and outer nuclear layers, such that cells with nuclei closest to the lens have earlier birthdates (brightest BrdU signal). (B) Pulsed BrdU labeling experiment. Math5>Cre; *ZAP* embryos were transiently exposed to BrdU at E15.5. Adult retinas were stained with hPLAP and BrdU antibodies and PNA lectin. *Math5+* cone (hPLAP+ PNA+ BrdU+, arrow) and bipolar (hPLAP+ BrdU+, arrowhead) cells are indicated. (C) Cone-rod ratio plots for birthdated hPLAP*+* (red), hPLAP− (blue) and combined (black) photoreceptor groups. The ratio of cone-to-rod births decreases steadily between E14.5 and E17.5 for hPLAP*+* and hPLAP-populations. The curves are parallel, indicating that the fate of *Math5+* cells changes over time, similar to other retinal progenitors. However, the cone-to-rod ratio is 3-fold higher for *Math5+* progenitors at every time point, suggesting that these cells have a fixed cone vs. rod bias, or are shifted by 0.5 days, compared to other neurogenic cells (hPLAP−) in the same retinal environment. (D) Cone-rod ratio plot for birthdated GFP+ (red), GFP− (blue) and combined (black) photoreceptor groups in *Math5* −/−; Math5>Cre; R26*flox*GFP mice. Scale bar, 50 m.

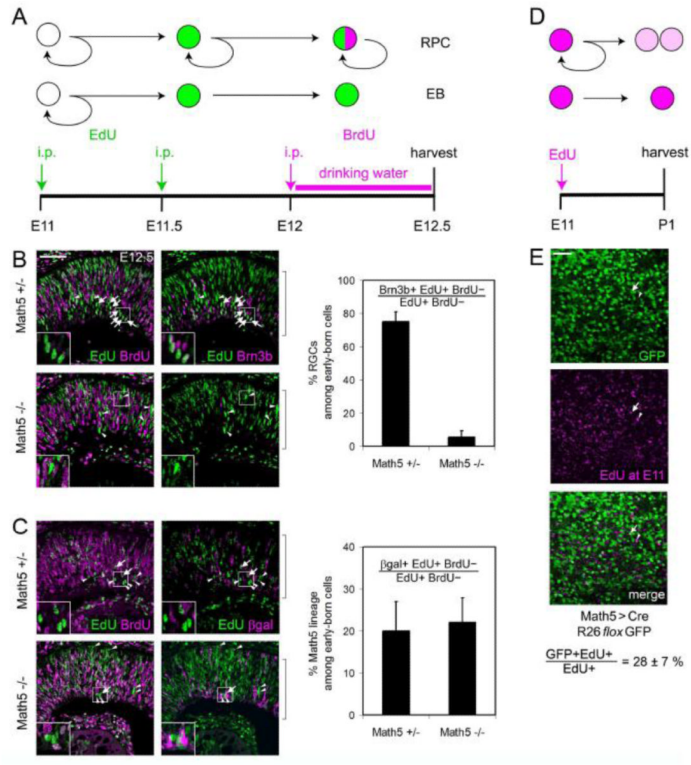

Fig. 6.

Math5 marks many of the earliest born cells in the retina. (A-C) Window labeling analysis. (A) Embryos were exposed to pulses of EdU at E11 (onset of neurogenesis) and E11.5, and to continuous BrdU from E12 to E12.5. Progenitors (RPCs) that continue to cycle through E12.5 are EdU+ BrdU+, while cells that have exited mitosis between E11 and E12 are EdU+ BrdU-, and represent the earliest born cohort of retinal neurons. (B-C) Sections through the neural retina (brackets). (B) Most early-born cells in *Math5* +/− mice adopt RGC fate (EdU+ BrdU-Brn3b+, arrows). The Brn3b-cells in this cohort are likely to include horizontal cell precursors (arrowheads). Few Brn3b+ RGCs (arrows) are present in Math5 −/− embryos, and the abundance of non-RGC fates increases accordingly (arrowheads). (C) Early-born *Math5-lacZ* (EdU+ BrdU-βgal+, arrows) and βgal− (arrowheads) cells are shown in *Math5* +/− (top) and *Math5* −/− (bottom) mice. Only ~20% of the early-born cohort expresses the *Math5* transcription unit (βgal+), in both genotypes. (D-E) Birthdating analysis. (D) E11 Math5>Cre; R26*flox*GFP embryos were exposed to a single EdU injection and analyzed at P1. (E) Flatmounted retinas were stained for EdU and GFP and imaged through the GCL. Strongly EdU+ cells mark the earliest born retinal neurons. Confocal projection image (6-10 μm) shows EdU+ GFP+ (arrow) and EdU+ GFP− (arrowhead) cells. Only 28% of the GCL cells born at E11 are in the Math5+ lineage. i.p., intraperitoneal; EB, early-born. Error bars represent the binomial standard deviation. Scale bar, 50 m.

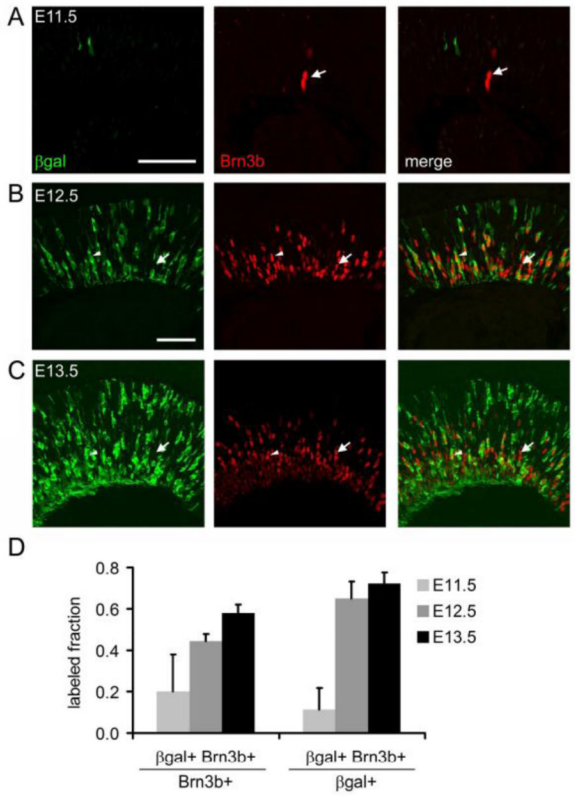

Fig. 7.

A subset of Brn3b+ RGCs derives from the *Math5* lineage. (A-C) Sections from embryonic *Math5-lacZ*/+ retinas co-stained for βgal and Brn3b. At E11.5, relatively few Brn3b+ cells are βgal+ (A, arrow). The fraction of Brn3b+ cells expressing *Math5-lacZ* (arrowheads) increases from E12.5 (B) to E13.5 (C). However, there are many *Math5*-independent RGCs (arrows) at each age. (D) Histograms showing the fraction of *Math5*+ cells among Brn3b+ RGCs and the fraction of Brn3b+ RGCs within the *Math5*+ cohort. Error bars show the standard deviation (n = 3 sections). The total number of cells counted at E11.5, E12.5 and E13.5 was 13, 228 and 667, respectively. Scale bar, 50 μm.

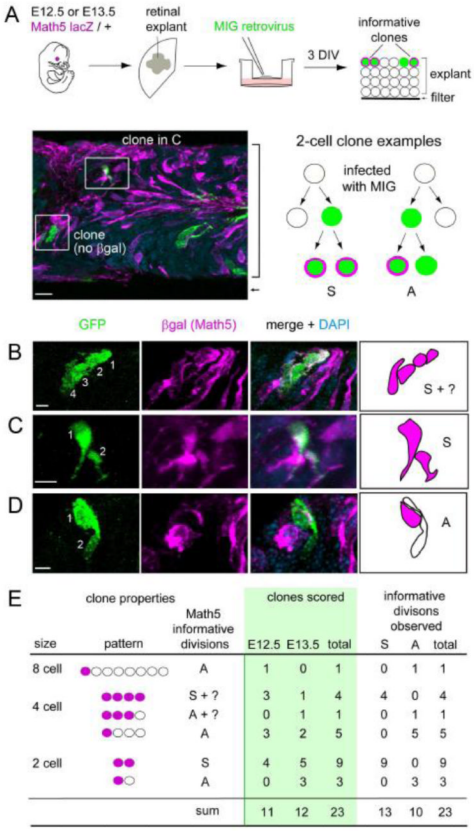

E

clone properties		Math5 informative divisions	clones scored			informative divisons observed		
size	pattern		E12.5	E13.5	total	S	A	total
8 cell	●○○○○○○○	A	1	0	1	0	1	1
4 cell	●●●●	S + ?	3	1	4	4	0	4
	●●●○	A + ?	0	1	1	0	1	1
	●○○○	A	3	2	5	0	5	5
2 cell	●●	S	4	5	9	9	0	9
	●○	A	0	3	3	0	3	3
		sum	11	12	23	13	10	23

Fig. 8.

Retrovirally marked clones exhibit symmetric and asymmetric patterns of *Math5* expression. (A) E12.5 or E13.5 retinas were explanted from *Math5 lacZ/+* embryos, flattened on polycarbonate membranes, infected at low density with a retroviral stock to mark clonal lineages (green), and cultured for 3 days *in vitro* (DIV). The micrograph shows a cross-section from a representative explant (bracket) co-stained for cytoplasmic βgal (magenta) and GFP (green). The diagram shows hypothetical 2-cell clone with βgal+ cells. Each clone reflects one informative terminal division: a symmetric [S] division which gave rise to two *Math5+* daughters (left); or an asymmetric [A] division, which gave rise to one *Math5+* and one *Math5-* daughter (right). (B-D) Confocal Z-stack projections and drawings showing representative clones that are symmetric (B, C) or asymmetric (D) with respect to *Math5* expression. (E) Summary of observed clones containing at least one *Math5+* cell. Informative divisions have a unique interpretation, and give rise to one [A] or two [S] *Math5+* daughters. Both types of divisions were identified. MIG, MSCV-IRES-GFP virus. Scale bars: 10 m in A; 5 m in B-D.

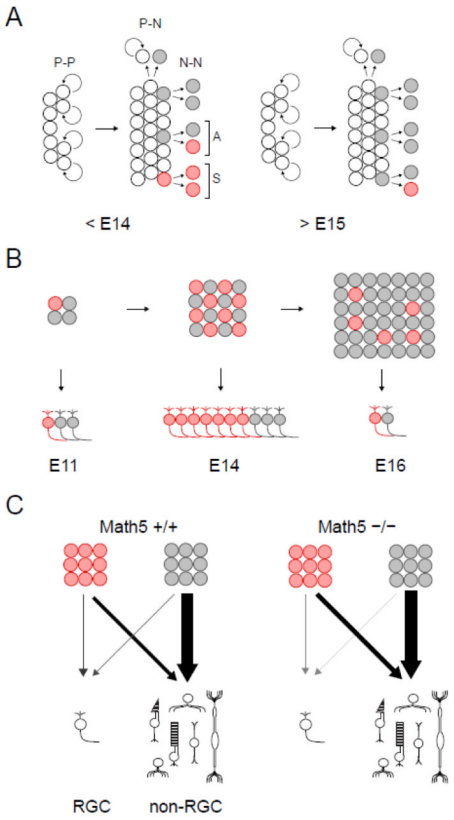

Fig. 9.

Natural history of the *Math5* lineage. (A) The timing of *Math5* expression shifts during retinal histogenesis. RPCs (white) shift from a proliferative (P-P) mode of division to stem (N-P) or terminal (N-N) modes, giving rise to neurogenic cells (gray). These express *Math5* (red) either during (S, symmetric) or after (A, asymmetric) final mitosis. During early retinal development (<E14), *Math5* is frequently expressed during G2 phase of the last cell cycle, generating two *Math5*+ daughters. During later stages (>E15), *Math5* is exclusively expressed by post-mitotic cells. (B) The size of the neurogenic (birthdated) population and proportion of *Math5*+ cells changes during development. At the onset of neurogenesis (E11), *Math5* is expressed by 20-30% of newborn cells. The number of *Math5*+ cells peaks during midgestation (E14) and rapidly diminishes (E16), while the neurogenic population as a whole continues to expand. The temporal profile for RGC birthdates follows similar kinetics, and reflects *Math5*+ and *Math5*− populations. (C) The fate spectrum of *Math5* lineage (red) and other neurogenic (gray) cells in wild-type and mutant mice. The thickness and shading of arrows denotes the relative demographic contribution of these cohorts to the mature retina.

Table 1

Cell type distribution of Math5 lineage descendants In wild-type Math5>Cre transgenic retinas

	cells counted					
	Math5 lineage	total	Math5 lineage (% of cell type)[§]	cell type[†] (% of retina)	Math5 lineage (% of retina)	cell type[‡] (% of Math5 lineage)
CELL TYPE	(*a*)	(*b*)	(*a*/*b*) × 100	(*c*) × 100	(*a*/*b*)(*c*) × 100	(*a*/*b*)(*c*/*f*) × 100
RGC	700	1,265[#]	55[§]	0.6	0.3	11
cone	1,515	4,914	31	22	0.7	23
horizontal	1,041	3,592	23	0.5	0.2	5
amacrine	1,665	15,570[*]	11	7.9	0.8	29
INL	1,198	13,920[*]	9	7.0	0.6	20
displaced	467	1,648[#]	28	0.9	0.2	8
rod	2,085	173,000[*]	1	78.5	0.9	32
bipolar	12	12,900[*]	<0.1	7.4	<0.005	<0.2
Müller glia	5	8,800[*]	<0.1	2.9	<0.002	<0.1
TOTAL				**100.0**	**2.9(*f*)**	**100**

RGCs, displaced amacrines, and INL amacrines were counted in 33 fields (200×,8 eyes. 6 mice. R26*flox*GFP reporter). Horizontal cells were counted in 58 sections (8 eyes,6 mice, R26*FLOX*GFP reporter). All other cell types were counted in 50 to 70 fields (200X, 16 eyes, 12 mice, Z/AP reporter) Math5+ descendants detected using the Cre lineage system comprise 2.9% of the adult retina (*f*).

[*] Estimated using cell type ratios reported by Jeon *et al.* (1998) for adult C57BL/6J mice. The total number of cones counted in surveyed fields was multplied by 35.2 to give the numberof rods, and by 3.32 for bipolar cells and 1.3 for muüller glia The total number of GCL neurons surveyed (RGC and displaced amacrines) was multiplied by 4.78 to estimate the number of inner nuclear layer (INL) amacrines.

[#] RGCs (identified by retrograde axon labeling) represent 43% of GCL neurons (1265/2913 cells). The remaining GCL cells were scored as displaced amacrines.

[§] Among $n = 8$ eyes, the mean RGC labeling fraction ±SEM was 54 ±2%, with a range between 46 and 63%. The overall labeling fraction for the GCL was 40% (1167/2913 cells), which represents 24% RGCs(700/2913 cells)and 16% displaced amacrines (467/2913 cells).

[†] Calculated from Jeon *et al.* (1998) and shown in Fig 3I (left pie chart)

[‡] These values are shown in Fig 3I (middle pie chart).